The Early Radiation of Sauropodomorphs in the Carnian (Late Triassic) of South America

Max C. Langer, Júlio C. A. Marsola, Rodrigo T. Müller, Mario Bronzati, Jonathas S. Bittencourt, Cecilia Apaldetti, and Martín D. Ezcurra

Abstract Carnian (Late Triassic) deposits of South America provide the oldest unequivocal dinosaur records worldwide, most of which has been assigned to the sauropodomorph lineage. This includes *Eoraptor lunensis*, *Panphagia protos*, and *Chromogisaurus novasi*, from the Ischigualasto Formation, Argentina, and *Saturnalia tupiniquim*, *Pampadromaeus barberenai*, *Buriolestes schultzi*, and *Bagualosaurus agudoensis*, from the Santa Maria Formation, Brazil. Here, we

Electronic supplementary material The online version contains supplementary material available at (10.1007/978-3-030-95959-3_1).

M. C. Langer (✉) · M. Bronzati
Departamento de Biologia, FFCLRP, Universidade de São Paulo, Av. Bandeirantes 3900 Ribeirão Preto 14040-190, Brazil
e-mail: mclanger@ffclrp.usp.br

J. C. A. Marsola
PPG Biologia Animal, IBILCE, Universidade Estadual Paulista, R. Cristóvão Colombo 2265 São José do Rio Preto 15054-000, Brazil

Departamento de Biologia e Zootecnia, FEIS, Universidade Estadual Paulista, R. Monção 226, Ilha Solteira 15385-000, Brazil

R. T. Müller
Centro de Apoio à Pesquisa Paleontológica da Quarta Colônia, Universidade Federal de Santa Maria, R. Maximiliano Vizzotto 598, São João do Polêsine 97230-000, Brazil

J. S. Bittencourt
Departamento de Geologia, Universidade Federal de Minas Gerais, Av. Antônio Carlos 6627, Belo Horizonte 31270-901, Brazil
e-mail: jsbittencourt@ufmg.br

C. Apaldetti
Consejo Nacional de Investigaciones Científicas y Técnicas (CONICET), Instituto y Museo de Ciencias Naturales, Universidad Nacional de San Juan, Avenida España 400 Norte, San Juan 5400, Argentina

M. D. Ezcurra
Consejo Nacional de Investigaciones Científicas y Técnicas (CONICET), Museo Argentino de Ciencias Naturales 'Bernardino Rivadavia', Av. Ángel Gallardo 470, Buenos Aires C1405DJR, Argentina

A. Otero et al. (eds.), *South American Sauropodomorph Dinosaurs*, Springer Earth System Sciences, https://doi.org/10.1007/978-3-030-95959-3_1

demonstrate that their holotypes anatomically differ from one another, supporting the taxonomic validity of the species. In addition, a morphological disparity analysis, with significant statistical support, clustered some of the better-known specimens of *E. lunensis*, *Sat. tupiniquim*, and *Bu. schultzi*, with the respective holotypes. For the latter two taxa, this was corroborated by a specimen-level phylogenetic analysis that also found *Ba. agudoensis* as the sister taxon to post-Carnian sauropodomorphs. Our results also suggest that *Bu. schultzi* and *E. lunensis* are the earliest branching sauropodomorphs and that *Sa. tupiniquim* and *Pam. barberenai* are closer to Bagualosauria. A species-level phylogenetic analysis further suggests that *Bu. schultzi* and *E. lunensis* form a clade, that *Sa. tupiniquim* is the sister taxon to Bagualosauria, and that *Pan. protos* and *Ch. novasi* are also more highly nested, forming a clade with *Pam. barberenai.*

Keywords Dinosauria · Sauropodomorpha · Bagualosauria · Ischigualasto formation · Santa Maria formation

1 Introduction

Research on Carnian (early Late Triassic) sauropodomorphs started about twenty years ago with the description of *Saturnalia tupiniquim* from south Brazil (Langer et al. 1999). Because coeval dinosaurs known at the time were either assigned to Ornithischia (*Pisanosaurus mertii*) or Theropoda (*Eoraptor lunensis*), or had unclear affinities (herrerasaurids), Sauropodomorpha was until then the only of the three major dinosaur lineages lacking an Ischigualastian (≈Carnian; Langer 2005; Langer et al. 2018) record. Funny enough, the present knowledge reveals that the most abundant Carnian dinosaurs were sauropodomorphs (including the 'ex-theropod' *E. lunensis*), whereas the record of coeval ornithischians and theropods is meagre. In fact, the Carnian diversity of the latter clades may have been even reduced, as neither group has currently undisputed representatives of that age (see Novas et al. 2021). This is because the putative theropod affinity of herrerasaurs continues under debate (e.g. Pacheco et al. 2019), as it is also the case for the affinities of *Nhandumirim waldsangae* and *Eodromaeus murphi* to that group (e.g. Langer et al. 2017; Pacheco et al. 2019) and the ornithischian affinity of *Pi. mertii* (e.g. Agnolin and Rosadilla 2018; Baron et al. 2017a).

Carnian sauropodomorphs recognised after *Sat. tupiniquim* (Fig. 1) were described in the last ten years or so (Martínez and Alcober 2009; Ezcurra 2010; Cabreira et al. 2011, 2016; Pretto et al. 2019), namely *Panphagia protos*, *Chromogisaurus novasi*, *Buriolestes schultzi*, *Pampadromaeus barberenai*, and *Bagualosaurus agudoensis.* The latter three were found in the Alemoa Member of the Santa Maria Formation, in south Brazil, which also yielded *Sat. tupiniquim.* The former two came from the Ischigualasto Formation, north-western Argentina, along with *E. lunensis*, a taxon that since the proposal of Martínez et al. (2011) has been most frequently accepted as belonging to Sauropodomorpha. Both stratigraphic units

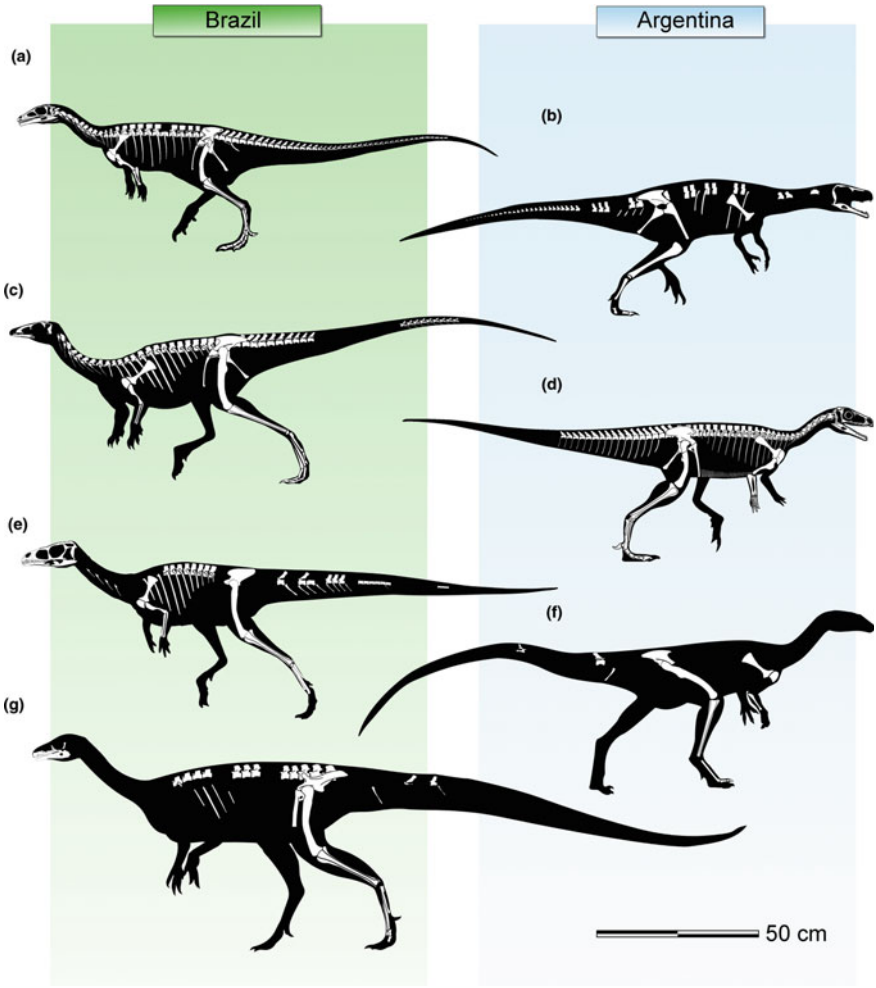

Fig. 1 Sauropodmorph diversity on the Carnian of South America. **a** *Buriolestes schultzi* (modified from artwork of MS Garcia following Cabreira et al. 2016). **b** *Panphagia protos* (modified from Martínez and Alcober 2009). **c** *Saturnalia tupiniquim* (modified from artwork of MS Garcia following Langer 2003). **d** *Eoraptor lunensis* (modified from artwork of MS Garcia following Sereno et al. 2012). **e** *Pampadromaeus barberenai* (modified from artwork of MS Garcia following Langer et al. 2019). **f** *Chromogisaurus novasi* (modified from artwork of DH Heman following Müller et al. 2020). **g** *Bagualosaurus agudoensis* (modified from artwork of MS Garcia following Pretto et al. 2019)

have been dated based on radioisotopic studies (Rogers et al. 1993; Martínez et al. 2011, 2012a; Langer et al. 2018; Desojo et al. 2020; Colombi et al. 2021), all of which agree on a late Carnian age for their main dinosaur-bearing beds; 231–229 Ma for the lower Ischigualasto Formation and ca. 233 Ma for the upper Santa Maria Formation.

Following an original proposal by Salgado et al. (1997), some authors (e.g. Langer 2003; Langer et al. 2010; see also Sereno 1998) employed node-based definitions for Sauropodomorpha that, based on most phylogenetic arrangements so far proposed, would exclude the Carnian members of the lineage. The alternative maximal-clade (i.e. stem-based) definitions (Upchurch 1997; Galton and Upchurch 2004) better fit the most common usage of the term (Sereno et al. 2005), including such early branching Carnian taxa, and this was fixed by Fabbri et al. (2020) in *Phylonyms*. Indeed, as current phylogenetic studies mostly concur in placing the seven taxa that form the core of this revision closer to *Saltasaurus loricatus* than to either *Allosaurus fragilis* or *Iguanodon bernissartensis*, they should, by definition, be referred to as sauropodomorphs. In fact, the understanding that such Carnian taxa belong to Sauropodomorpha broke some paradigms about the paleobiology of the early representatives of the group, hitherto inferred based on 'prosauropod-grade' taxa, as relatively large-sized, small-headed, long-necked, omnivore/herbivore, and facultatively quadruped animals. The Carnian forms revealed that none of those typically sauropodomorph traits was present in the earliest radiation of the group, which was represented by small, lightly build animals that had larger heads and shorter necks, and were most probably faunivorous and fully biped (Bronzati et al. 2017).

After an original suggestion by Bonaparte et al. (1999), Ezcurra (2010) proposed that the Norian dinosaur *Guaibasaurus candelariensis* nested, along with some Carnian taxa, into a clade of early sauropodomorphs named Guaibasauridae. In addition, Ezcurra (2010) proposed that *Sat. tupiniquim* and *Ch. novasi* formed a minimal clade named Saturnaliinae. These suggestions were followed by some authors (e.g. Novas et al. 2011; Baron et al. 2017b; Cau 2018), whereas others allied *Gu. candelariensis* to theropods (Yates 2017a, b; Langer et al. 2011; Marsh et al. 2019). This gave rise to the notion that at least some Carnian sauropodomorphs form a clade, either including *Gu. candelariensis* or not, exclusive of most younger members of the group (e.g. Martínez et al. 2011; Langer et al. 2017; Baron et al. 2017b; Müller et al. 2018a). Instead, other studies recover a more pectinate phylogenetic pattern for early sauropodomorph radiation (e.g. Martínez et al. 2012b; Cabreira et al. 2016; Pretto et al. 2017; Müller et al. 2018a), and intermediate arrangements have also been proposed. For example, a clade including part of the Carnian sauropodomorph diversity was termed Saturnaliidae by Langer et al. (2019), translated from Saturnaliinae Ezcurra (2010), whereas its sister clade was named Bagualosauria. The latter clade includes a single Carnian taxon, the name-bearing *Ba. agudoensis* (Pretto et al. 2019). The phylogenetic study proposed here will tackle the relations of several 'guaibasaurids', but will not investigate the possible sauropodomorph affinity of *Gu. candelariensis*. A broader sample of saurischians are required to properly evaluate that possibility, which is beyond the scope of this work. For the same reasons, the recent proposals that (1) most Carnian 'sauropodomorphs' nest outside of

Eusaurischia (Pretto et al. 2019), (2) the putative theropod *Nh. waldsangae* (Marsola et al. 2018) may belong to Saturnaliidae (Pacheco et al. 2019), and (3) the still often suggested non-sauropodomorph affinity of *E. lunensis* will not be tested here.

So far, Carnian sauropodomorphs were positively recognised only in South America. A possible exception corresponds to a partial femur from the Pebbly Arkose Formation of Zimbabwe (Raath 1996), which Langer et al. (1999) suggested to be closely allied to *Sat. tupiniquim* and Ezcurra (2012a) considered an indeterminate saurischian. More recently, further dinosaur material coming from that stratigraphic unit was reported by Griffin et al. (2018), including a partial skeleton with sauropodomorph affinities. The confirmation of this find would highlight the similarities of that African paleofauna to those of 'Ischigualastian' deposits of South America, as already inferred (Langer et al. 2018) by the presence of the rhynchosaur *Hyperodapedon*. Another likely coeval stratigraphic unit (Langer 2005), the lower Maleri Formation of India, yielded the controversial dinosaur *Alwalkeria maleriensis* (Chatterjee 1987). As previously discussed (Langer 2004; Remes and Rauhut 2005; Novas et al. 2011; Ezcurra 2012a), this taxon shares several traits with early sauropodomorphs, but its fragmentary and chimeric nature hampers a proper evaluation of its affinities. Also from India, but from the younger (possibly Norian) upper Maleri Formation, Novas et al. (2011) described a fragmentary specimen (ISI R277) that may belong to Guaibasauridae. Finally, the only proposed non-Gondwanan record of the group corresponds to *Agnosphitys cromhallensis* (Fraser et al. 2002; Ezcurra 2010). Yet, this hypothesis was mostly abandoned lately, given the composite nature of the taxon and its position in more recent phylogenetic studies (e.g. Baron et al. 2017a, b; but see Chapelle et al. 2019). Hence, except for the still undescribed Zimbabwean form, all other non-South American putative guaibasaurids and/or Carnian sauropodomorphs are very controversial, residing outside the scope of the present work, which is to evaluate in detail the alpha-taxonomy and relations of the better-known South American members of the group.

Recently, Baron et al. (2017a, b) assigned the putative dinosaur *Nyasasaurus parringtoni* from the Middle Triassic Lifua Member of the Manda beds of Tanzania (Nesbitt et al. 2013) to Sauropodomorpha. Yet, as fully discussed by various authors (Langer et al. 2017; Ezcurra et al. 2017; Novas et al. 2021), both the affinities of *Ny. parringtoni* and age of the Manda beds are controversial, and this taxon is not discussed further here.

The description of five new taxa in a ten-year interval raised questions about possible synonymies among the Carnian sauropodomorphs of Brazil and Argentina (Langer et al. 2019; Müller and Garcia 2019): are they really different from one another, or could this be a case of taxonomic inflation? In an attempt to tackle this and other questions, we present below a brief review of the status of each of the seven South American Carnian sauropodomorphs, followed by phylogenetic and Principal Coordinates Analysis, aimed to better understand their morphological diversity. In the end, we hope to integrate these data to address the above-proposed question.

Institutional Abbreviations CAPPA/UFSM: Centro de Apoio à Pesquisa Paleontológica da Quarta Colônia, Universidade Federal de Santa Maria, São João do Polêsine, Brazil; **MACN**: Museo Argentino de Ciencias Naturales 'Bernardino Rivadavia', Buenos Aires, Argentina; **MCP**: Museu de Ciências e Tecnologia, Pontifícia Universidade Católica do Rio Grande do Sul, Porto Alegre, Brazil; **PUC/RS**: Pontifícia Universidade Católica do Rio Grande do Sul, Porto Alegre, Brazil; **PVSJ**: Museo de Ciencias Naturales, Universidad Nacional de San Juan, San Juan, Argentina; **UFRGS**: Universidade Federal do Rio Grande do Sul, Porto Alegre, Brazil; **ULBRA**: Universidade Luterana do Brasil, Canoas, Brazil.

2 Methods

2.1 Protocol for Building the Taxon-Character Matrix

Because we intended to design a phylogenetic study specifically to tackle the issue of Carnian sauropodomorph relationships, we conducted a simple protocol to extract information from the phylogenetic literature about the group. First, starting with Langer et al. (1999) and ending in June 2020, we identified all numerical phylogenetic studies that included, as terminal taxa, at least two of the seven early dinosaurs that form the core of this study. There were some exceptions, however, such as studies focused on pseudosuchians that employed modified versions of the Nesbitt (2011) data-matrix, which includes *E. lunensis* and *Sat. tupiniquim.* For these studies, we inferred that the part of the data that is of interest to the present revision was not modified in more recent iterations (at least not substantially), as the authors did not aim at investigating early dinosaur relations. Likewise, studies on theropods that employed modified versions of the data-matrix of Smith et al. (2007), which also includes *E. lunensis* and *Sat. tupiniquim*, were not selected for the second step of the protocol (see below). This first step resulted in the identification of 147 phylogenetic studies (see Supplementary Material) with suitable data-matrices.

The data-matrices of those 147 studies were then subject to a manual search for characters with variable scoring among the seven taxa discussed here, i.e. characters were selected if not scored equally (with the same state) for those taxa. In that search, missing entries were not considered different states; otherwise, the high number of such entries for incomplete taxa, such as *Ch. novasi*, would result in the selection of almost all characters in those matrices. Also, considering that characters that do not vary within those Carnian taxa could still be phylogenetically informative, because they could support their nesting in a single clade, sister to younger sauropodomorphs, e.g. Müller et al. (2018a), we expanded the search for variable characters to other early branching members of the group, including the genera *Pantydraco*, *Thecodontosaurus*, *Efraasia*, *Macrocollum*, and *Plateosaurus*, regardless of their specific assignments. This expanded search resulted in a selection of over 3,500 variable characters, which were then manually compared in search for

the multiple expected overlapping/duplication among them. Purged of the duplications, a list of nearly 800 non-overlapping characters was built. Their definitions were standardised, mostly following the grammar of Sereno (2007b), when the characters themselves and their compartmentations in different states were revised for clarity, avoiding ambiguous statements. In addition, new characters gathered from the comparisons conducted in Sect. 3.1, were included. All characters were then scored de novo based on first-hand observations of all terminals. During the scoring process, improvements to character definition and state compartmentation were identified and incorporated into the character list without further ado. In addition, despite being originally scored as variable for the selected taxa in data-matrices gathered for this revision, some characters patently refer to anatomical traits that are unseen among early sauropodomorphs and were excluded from the final list. This included, for example, the presence of nasal crests, of an otic incisure, a double-headed ectopterygoyd, a caudodorsal process in the lacrimal, a transverse ridge along the basioccipital/parabasisphenoid articulation, caniniform teeth, and pneumatised nasal, articular, and ectopterygoid, among others. We also excluded characters with very ambiguous definitions, in particular those dealing with traits of serially homologous elements (e.g. vertebrae, teeth) with variable conditions, but lacking more precise indication about which individual elements were under evaluation. This all resulted in a data-matrix with 771 characters (see Supplementary Material), which was employed in the analysis.

The selection of terminals followed the taxonomic revision provided in the following sections, where the uniqueness of all Carnian sauropodomorph holotypes was corroborated, confirming the validity of the taxa typified by them. These were included in the data-matrix following two strategies. Firstly, the seven holotypes, as well as five other specimens of *E. lunensis*, *Sat. tupiniquim*, and *Bu. Schultzi,* were scored separately, but composite terminals of these three species were then built based on the conjoined scoring of the specimens originally attributed to them. Such composite terminals were scored multistate when two or more states were positively identified for the individual specimens it represents. On the other hand, if one of the specimens was scored multistate and a single state was given to the others, that state was assigned to the composite terminal.

Another premise of the protocol was that the seven taxa that form the core of the study are members of the sauropodomorph branch of dinosaurs. Clearly, that was not the case for *E. lunensis* in the first studies to include the taxon, and it is fair to say that this is still not a completely settled issue (see below). Yet, we opted to follow this premise so that we could focus our efforts on investigating the relations among those putative early sauropodomorphs. Likewise, we assumed that such Carnian taxa are all external to the minimal clade formed by all known post-Carnian sauropodomorphs, which are represented in the data-matrix by *Pantydraco caducus*, *Efraasia minor*, *Plateosaurus engelhardti*, and *Macrocollum itaquii*. On the other hand, the outgroup taxa include the herrerasaurids *Herrerasaurus ischigualastensis* and *Gnathovorax cabreirai*, the possible herrerasaurian *Tawa hallae*, and the neotheropod *Coelophysis bauri*, as well as the non-dinosaur dinosauromorph *Lewisuchus admixtus*, which

was used to root the topologies. The final taxon-character matrix, with 771 characters scored for 24 terminals—five outgroup taxa, twelve Carnian specimens, three composite Carnian taxa, and four Norian taxa—can be seen in the Supplementary Material.

2.2 Tree Search Strategy and Branch Support/Stability

The data-matrix was analysed using both the composite scorings for *E. lunensis*, *Sat. tupiniquim*, and *Bu. schultzi* ('combined' analysis) and their type and referred specimens as independent terminals ('specimen-based' analysis). The analyses were conducted under equally weighted parsimony using TNT 1.5 (Goloboff et al. 2008; Goloboff and Catalano 2016). Heuristic search of 1,000 replications of Wagner trees (with random addition sequence) followed by TBR branch swapping (holding ten trees per replicate) was performed. Branches with a maximum possible length of zero among any of the recovered most parsimonious trees (MPTs) were collapsed (rule 3 of Swofford and Begle 1993; Coddington and Scharff 1994). Based on the two premises outlined in the previous section, we applied constrains using an a priori built tree that forced the monophyly of post-Carnian sauropodomorphs and Sauropodomorpha. The following multistate characters were ordered because they represent nested sets of character states: 1, 13, 14, 23, 27, 43, 49, 56, 63, 71, 72, 73, 89, 91, 94, 97, 109, 120, 135, 137, 163, 165, 173, 174, 176, 177, 190, 195, 197, 214, 219, 221, 224, 237, 269, 271, 274, 275, 276, 282, 284, 299, 300, 302, 314, 341, 343, 344, 345, 352, 358, 370, 379, 382, 383, 384, 385, 393, 394, 398, 407, 415, 429, 439, 446, 454, 455, 461, 462, 463, 472, 477, 478, 486, 501, 504, 509, 518, 520, 524, 552, 557, 562, 564, 587, 588, 593, 596, 601, 606, 609, 612, 613, 616, 618, 623, 640, 643, 659, 660, 668, 676, 681, 690, 692, 693, 695, 701, 718, 719, 731, 744, 762, 766, 767, and 768. Consistency and retention indices were calculated considering only those terminals active during the tree search (using the 'maxstepsact' function), in a modified version of the STATS.RUN script. After the tree searches, the possible occurrence of topologically unstable terminals was tested using the iterPCR protocol (Pol and Escapa 2009). As a measure of branch support, decay indices (=Bremer support) were calculated (Bremer 1988, 1994) and, as a measure of branch stability, a bootstrap resampling analysis (Felsenstein 1985) was conducted, with 10,000 pseudo replications. Both absolute and GC (i.e. difference between the frequency whereby the original group and the most frequent contradictory group are recovered in the pseudo replications; Goloboff et al. 2003a, b) bootstrap frequencies were reported. Analyses forcing topological constraints were conducted to find the minimum number of steps necessary to force alternative suboptimal positions for the Carnian sauropodomorph specimens or species.

2.3 Morphological Disparity Analysis

The morphological diversity (disparity) of the Carnian sauropodomorph specimens was quantified based on the matrix of discrete characters described above (excluding the combined terminals for *E. luensis*, *Sat. tupiniquim*, and *Bu. schultzi*). A distance matrix was generated from the taxon-character matrix using the Maximum Observable Rescaled Distance (MORD) (Lloyd 2016; see Lehmann et al. 2019) with the R package Claddis v0.6.1 (Lloyd 2016). An ordination of the distance matrix was performed using a Principal Coordinates Analysis (PCoA) without the necessity of trimming specimens before the analysis. We conducted the PCoA using the Lingoes correction because of the presence of negative eigenvalues. Subsequent Permutational Multivariate Analysis of Variance (PERMANOVA) and Linear Discriminant Analysis (LDA) based on the results of the PCoA used the first three coordinates (58.46% of accumulated variance), which were chosen after detecting the first major break of slope in the scree plot of explained variances. These two analyses were conducted in order to determine if the hypodigms of *E. luensis*, *Sat. tupiniquim*, and *Bu. schultzi* could be statistically differentiated from one another. In order to test if the morphospace distribution was significantly driven by body size, we conducted a generalised least squares regression between the values of the first three PCos and the logarithm of femoral length (as a proxy of body size) of each specimen.

3 Systematic Palaeontology

Dinosauria Owen 1842 [Langer et al. 2020].

Saurischia Seeley 1888 [Gauthier et al. 2020].

Sauropodomorpha Huene 1932 [Fabbri et al. 2020].

Eoraptor Sereno, Forster, Rogers and Moneta 1993

E. lunensis Sereno, Forster, Rogers and Moneta 1993

Holotype The holotype of *E. lunensis* (PVSJ 512) corresponds to a fairly complete skeleton of a probable young adult approaching skeletally maturity (Sereno et al. 2012). This is one of the most complete Carnian dinosaur skeletons known to date, lacking only most of the scapula, the coracoid, and manual phalanges from the left side and caudal vertebrae distal to the 17th position (Sereno et al. 1993, 2012).

Referred Specimens The referred specimens of *E. lunensis* (Sereno et al. 2012) include rather incomplete partial skeletons (PVSJ 559, 745, 860, 862), as well as isolated bones (PVSJ 852, 855, 876), from inferred adult (PVSJ 559, 855, 860, 876) and subadult (PVSJ 745, 852, 862) individuals (Table 1).

Table 1 List of specimens attributed to the Carnian sauropodomorphs of South America

Taxon/specimens	Parts preserved and maturity
Eoraptor lunensis	
PVSJ 512 (holotype)	Articulated skeleton including the skull and most of the postcranium, lacking most of left scapulocoracoid, most of left manual phalanges, and vertebral elements distal to caudal vertebra 17 (Sereno et al. 2012)
PVSJ 559 (referred material)	Two cranial trunk vertebrae, rib shafts, partial right hind limb, including a femur lacking the head, tibia, distal half of the fibula, astragalus, calcaneum, and metatarsal fragments (Sereno et al. 2012)
PVSJ 745 (referred material)	Partial basicranium, including basioccipital and parabasisphenoid, postaxial cervical vertebrae, multiple trunk, sacral, and caudal vertebrae, sacral rib, partial ilia, ischia, femora, and fibulae, distal end of tibia, and proximal portions of metatarsal II–IV (modified from Sereno et al. 2012; MDE pers. obs.)
PVSJ 852 (referred material)	Right femur (Sereno et al. 2012)
PVSJ 855 (referred material)	Right femur (Sereno et al. 2012)
PVSJ 860 (referred material)	Proximal and distal ends of left femur, distal end of right femur, proximal and distal ends of right tibia, proximal end of left tibia, and proximal end of right fibula (Sereno et al. 2012)
PVSJ 862 (referred material)	Proximal end of right humerus, distal ends of both femora, distal end of right tibia, proximal end of right fibula, and right astragalus (Sereno et al. 2012)
PVSJ 876 (referred material)	Right femur lacking midsection (Sereno et al. 2012)
Saturnalia tupiniquim	
MCP 3844-PV (holotype)	Articulated postcranial skeleton including most of the presacral vertebral series, both sides of the pectoral girdle, right humerus, partial right ulna, right radius, both sides of the pelvic girdle with the sacral series, left femur and most of the right limb (Langer 2003)
MCP 3845-PV (paratype)	Partial skeleton including part of the skull with braincase, the natural cast of a mandibular ramus bearing teeth, presacral series including caudal cervical and cranial trunk vertebrae, both sides of the pectoral girdle, right humerus, right side of the pelvic girdle and most of the right hind limb (Langer 2003)
MCP 3846-PV (paratype)	Incompletely prepared skeleton, from which a partial tibia and foot, as well as some trunk vertebrae, are visible (Langer 2003)

(continued)

Table 1 (continued)

Taxon/specimens	Parts preserved and maturity
Panphagia protos	
PVSJ 874 (holotype)	Partial disarticulated skeleton including right nasal, prefrontal and prootic, left frontal, both parietals and quadrates, supraoccipital, rostral half of the left hemimandible, right hemimandible lacking the rostral tip of the dentary, one cranial and two caudal cervical vertebrae, four caudal trunk neural arches, one trunk centrum, first primordial sacral vertebra, two proximal, one proximal-middle, and 15 distal caudal vertebrae, left scapula, ilium, pubic apron, ischium and proximal half of probable metatarsal 4, right tibia, astragalus, metatarsal 3, and four pedal phalanges of uncertain position, one of which is an ungual (Martínez and Alcober 2009)
Chromogisaurus novasi	
PVSJ 845 (holotype)	Partial postcranial skeleton including one proximal and two middle caudal vertebrae, proximal haemal arch, glenoid region of left scapulocoracoid, proximal end of right ulna (sensu Ezcurra 2010; interpreted as the caudal end of a rhynchosaur right hemimandible by Martínez et al. 2012b), partial ilia and femora, right tibia, proximal end of left tibia, partial right fibula and proximal end of left fibula, partial left metatarsal II (sensu Ezcurra 2010; interpreted as right by Martínez et al. 2012b), articulated phalanges of—possibly left—pedal digit II (sensu Ezcurra 2010; alternatively interpreted as belonging to the right pedal digit III by Martínez et al. 2012b), and unidentified bone fragments (Ezcurra 2010; Martínez et al. 2012b)
Pampadromaeus barberenai	
ULBRA-PVT 016 (holotype)	Disarticulated partial skeleton including a semi-articulated cranium set with right premaxilla, maxilla, lacrimal, left palatine, and an indeterminate partial palatal bone; skull bones including right frontal, prefrontal, postorbital, and pterygoid, left nasal, parietal, jugal, squamosal, quadrate, and pterygoid; nearly complete left dentary, with possible portions of the angular and surangular; partial right dentary; semi-articulated set of postdentary bones of the right lower jaw including, angular, surangular, articular, and prearticular; left prearticular; vertebrae including atlas/axis complex, third neck vertebra, eleven trunk vertebrae, articulated pair of sacral vertebrae and ribs, and 17 tail vertebrae; various neck and trunk ribs and haemal arches; partial left scapula; right scapula, humerus, and ulna; partial ilia; proximal portion of the left ischium; femora, tibiae, and fibulae; left metatarsals I and II, partial right metatarsal II, partial metatarsals III, and right metatarsal IV; two phalanges (Langer et al. 2018)

(continued)

Table 1 (continued)

Taxon/specimens	Parts preserved and maturity
CAPPA/UFSM 0027 (referred material)	Left femur (Müller et al. 2016a)
CAPPA/UFSM 0028 (referred material)	Left femur (Müller et al. 2017a)
Buriolestes schultzi	
ULBRA-PVT280 (holotype)	Articulated skeleton including partial skull and both lower jaws and partial postcranium, including few presacral, three sacral and 42 tail vertebrae; left scapula and forelimb lacking most of the manus; paired ilia and ischia; partial left pubis; and a nearly complete left hindlimb (Cabreira et al. 2016)
CAPPA/UFSM 0035 (referred material)	Articulated skeleton including a nearly complete skull and lower jaws and partial postcranium, including complete vertebral column lacking the last sacral vertebra and the caudal series; partial left scapula and coracoid, a fragmentary left humerus, both ilia, the proximal portion of both pubes, the proximal portion of the right ischium, an almost complete right femur, a fragmentary left femur and partial right tibia and fibula, and some phalanges from the right pedal digits III and IV. (Müller et al. 2018a)
ULBRA-PVT289 (referred material)	Isolated right femur (Müller et al. 2018a)
ULVRA-PVT056 (referred material)	Associated elements including two cervical vertebrae, ilium, proximal portion of the pubis, and femur from the right side, plus some phalanges (Müler et al. 2018a)
CAPPA/UFSM 0179 (referred material)	An isolated axis (Müller et al. 2017b)
Bagualosaurus agudoensis	
UFRGS-PV-1099-T (holotype)	Semi-articulated skeleton, including partial skull and mandible, trunk vertebrae, sacrum and isolated caudal vertebrae, fragmented ribs, gastralia, isolated haemal arches, both ilia, right pubis, femora, tibiae, fibulae and partial left pes (Pretto et al. 2019)

Geographic and Stratigraphic Provenance The holotype and all specimens referred to *E. lunensis* were collected from the Cancha de Bochas and Valle Pintado sites, Hoyada de Ischigualasto, Ischigualasto Provincial Park, San Juan, Argentina (Fig. 2; Sereno et al. 2012). They were found in rocks corresponding to the La Peña, Cancha de Bochas, and Agua de la Peña members of the Ischigualasto Formation, belonging to the *Hyperodapedon-Exaeretodon-Herrerasaurus* biozone (Martínez et al. 2012a; Colombi et al. 2021). The maximum age of *E. lunensis* is constrained by a radioisotopic date of 231.4 ± 0.3 Ma close to the base of the Ischigualasto

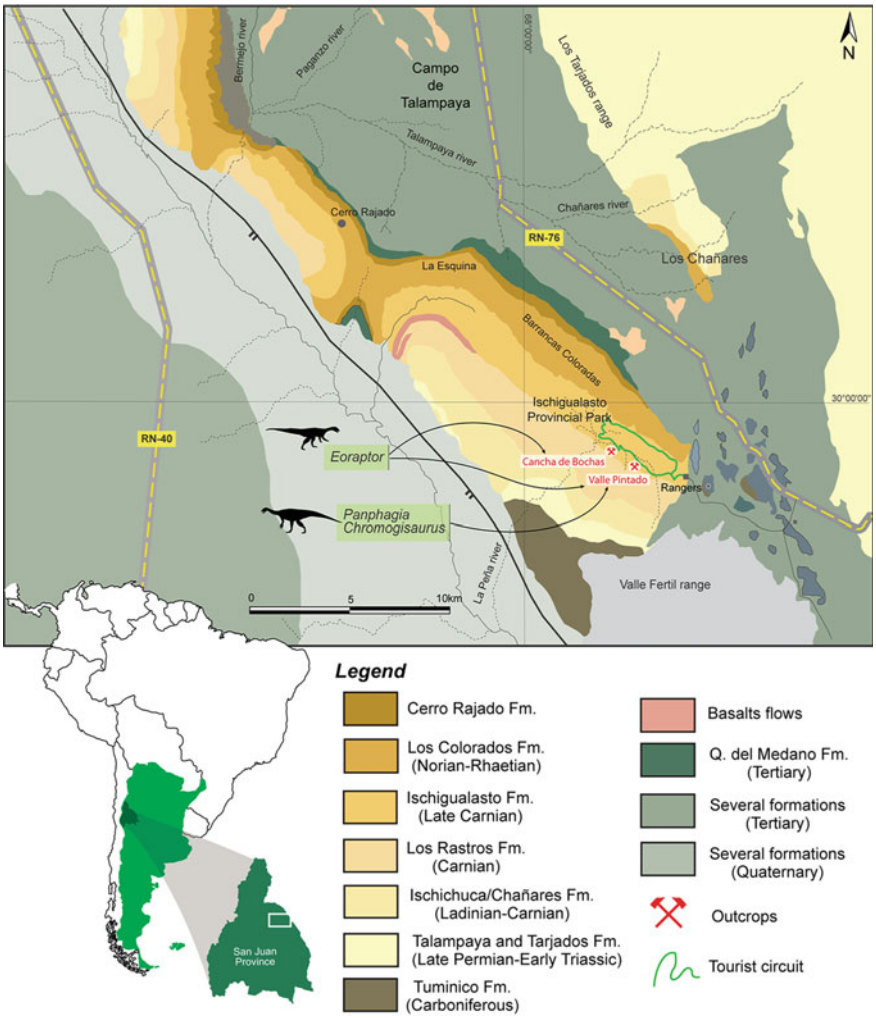

Fig. 2 Geological surface distribution map of the area around the Ischigualasto Provincial Park, San Juan, Argentina, indicating the sites where the specimens of *Eoraptor lunensis*, *Panphagia protos*, and *Chromogisaurus novasi* were found

Formation (Rogers et al. 1993). The upper stratigraphic range of that biozone, hence of *E. lunensis*, in the Provincial Park was constrained by an absolute age of 228.91 ± 0.14 Ma.

Proposed Phylogenetic Relations The first phylogenetic analysis to test the affinities of *E. lunensis* found the taxon as the earliest branching theropod, sister taxon to herrerasaurids plus neotheropods (Sereno et al. 1993). The theropod affinity of *E. lunensis* was supported by subsequent studies during the 1990s (e.g. Novas 1996; Sereno 1999). However, this interpretation started to be contradicted by some phylogenetic analyses in the beginning of this century, which found the species outside the theropod-sauropodomorph dichotomy (e.g. Langer 2004; Langer and Benton 2006; Upchurch et al. 2007; Yates 2017a, b; Nesbitt and Chatterjee 2008; Martínez and Alcober 2009; Alcober and Martínez 2010). Yet, other analyses continued to recover the more traditional theropodan position of *E. lunensis* (e.g. Ezcurra 2006, 2010; Ezcurra and Novas 2007; Nesbitt et al. 2009; Langer et al. 2011; Novas et al. 2011; Sues et al. 2011). More recently, a third alternative was proposed, this time placing *E. lunensis* as one of the earliest branching sauropodomorphs (Martínez et al. 2011). This hypothesis was supported by multiple subsequent studies (e.g. Ezcurra 2012b; Martínez et al. 2012b; Nesbitt and Ezcurra 2015; Cabreira et al. 2016; Baron et al. 2017a; Langer et al. 2017; Müller et al. 2018a; Marsola et al. 2018; Langer et al. 2019; Marsh et al. 2019; Pacheco et al. 2019; Ezcurra et al. 2020a; Müller and Garcia 2020; Pol et al. 2021), although a number of others carried on recovering theropodan affinities for *E. lunensis* (e.g. Martínez et al. 2012a; Baron and Barrett 2017; Baron et al. 2017b; Baron and Williams 2018). *Eoraptor lunesis* has been recovered in different positions among the earliest known sauropodomorphs, such as the earliest branching member of the group (e.g. Langer et al. 2019; Marsh et al. 2019), the sister taxon of all other sauropodomorphs with the exception of *Bu. schultzi* (e.g. Cabreira et al. 2016, 2018b; Pacheco et al. 2019; Müller and Garcia 2020; Garcia et al. 2021), within Saturnaliidae (e.g. Martínez et al. 2011; Müller et al. 2018a), or as one of the most immediate successive sister taxa to the Saturnaliidae plus Bagualosauria clade (Martínez et al. 2012b; Pol et al. 2021). In sum, a certain consensus was reached about the sauropodomorph affinities of *E. lunensis*; this position was recovered in most phylogenetic analyses published in the last ten years, and most of those that did not are based on datasets built during the first decade of this century. Yet, the position of *E. lunensis* among non-bagualosaur sauropodomorphs has been unstable.

General Anatomy and Paleobiology The anatomy of *E. lunensis* was described in detail by Sereno et al. (2012). The holotypic skeleton was estimated to be about 1.2 m long, with larger specimens (e.g. PVSJ 559) ca. 10% larger. The skull is about 0.8 times the femoral length, resembling the condition in most Carnian sauropodomorphs. It has a relatively large circular orbit, a slightly downturned premaxilla, but lacks a clear subnarial gap. The skull has four teeth in the premaxilla, 17 in the maxilla, and at least 20 in the dentary. Palatal teeth are present in the pterygoid. The marginal tooth crowns have a slight basal constriction and most are distally recurved, with the exception of those in the caudal part of the maxilla. 'Cheek-teeth' crowns have a rounded labial eminence and mesial and distal denticles/serrations. The

cervical vertebrae are moderately elongated, with a centrum length twice its height. The sacrum is composed of three vertebrae, one here reinterpreted as incorporated from the caudal series. The scapula has a relatively short and narrow blade with a moderately craniocaudal expanded end. The forearm is shorter than the relatively robust humerus, and the manus has five metacarpals, but only the first three digits have phalanges; although the fourth digit may have had or not a phalanx (Sereno et al. 2012). The manual ungual phalanges are slightly recurved. The pelvis has a partially opened acetabulum, an ilium with conspicuously developed pre- and postacetabular alae, and a pubis longer than the ischium. Femur and tibia are subequal in length, the former bearing an asymmetric fourth trochanter. The tibia has a short, laterally curved cnemial crest and the distal end is sub-squared, with a lateral groove separating a poorly developed caudolateral process from the facet for reception of the ascending process of the astragalus. Metatarsal III is the longest and metatarsal V the shortest, the latter lacking phalanges. Metatarsal I is slightly longer than half the length of metatarsal III and reaches the proximal end of the metatarsus.

Sereno et al. (2012) reviewed several palaeobiological aspects of *E. lunensis*, inferring that the antorbital fossa was occupied by an air sac emanating from the nasal cavity, but with no evidence of accessory diverticuli from the antorbital sinus. The rostrum was inferred to be akinetic, given the long suborbital ramus of the premaxilla and the premaxilla-maxilla contact lacking a significant diastema, but with a subnarial foramen. On the contrary, Sereno et al. (2012) suggested the presence of an intramandibular joint, with both dorsal and ventral articulations, allowing limited flexure on the vertical plane. Tooth crown anatomy—distal margins straight or only slightly concave in labial/lingual views, mesial margin with large (six per millimetre) and obliquely set denticles—was used to infer a pulping function suitable for plant matter, rather than a meat-cutting function. Also, Sereno et al. (2012) suggested the presence of a small keratinous beak at the rostral tip of the lower jaw, as indicated by the presence of neurovascular foramina and a retracted first dentary tooth. They also identified an extreme hollowing in some vertebrae, formed by internal cavities lacking pneumatic external communications. Traits of the cervical centra suggest that the neck formed a sigmoid curve, elevating the skull above the level of the trunk, with the ribs forming a flexible rod, ventrolateral and parallel to the centra. A forelimb shorter than half the hind limb length suggests that *E. lunensis* was biped, but the interosseous gap between the forearm bones, the long metacarpals 4 and 5, and the twisted phalanx 1 of the pollex precludes raptorial functions for the arm. The proportions among the hind limb parts (femur, epipodium, metatarsus), suggest more cursorial habits compared to Norian sauropodomorphs, but less than early ornithischians and theropods.

Saturnalia tupiniquim Langer et al. 1999

Holotype The holotype of *Sat. tupiniquim* (MCP 3844-PV) corresponds to an articulated partial skeleton (Table 1).

Reffered Specimens The two paratypes of *Sat. tupiniquim* (MCP 3845-PV and 3846-PV) are the only other specimens so far referred to that species (Langer et al.

1999). MCP 3846-PV is the less complete of them and MCP 3845-PV the only with cranial remains (Table 1).

Geographic and Stratigraphic Provenance The type-series of *Sat. tupiniquim* was collected in the site known as 'Cerro da Alemoa' or 'Waldsanga' (Langer 2005). This is located in the eastern outskirts of Santa Maria (Fig. 3), south of RS-509 road (coordinates: 29° 41′ 51.86″ S, 53° 46′ 26.56″ W). The site exposes the red mudstones of the Alemoa Member, Santa Maria Formation (Da Rosa 2015), overlaid by a basal fluvial conglomerate. MCP 3844-PV and 3845-PV were excavated about three metres below the conglomerate, whereas MCP 3846-PV was found three metres further down (Langer 2005). Between them (five metres below the conglomerate)

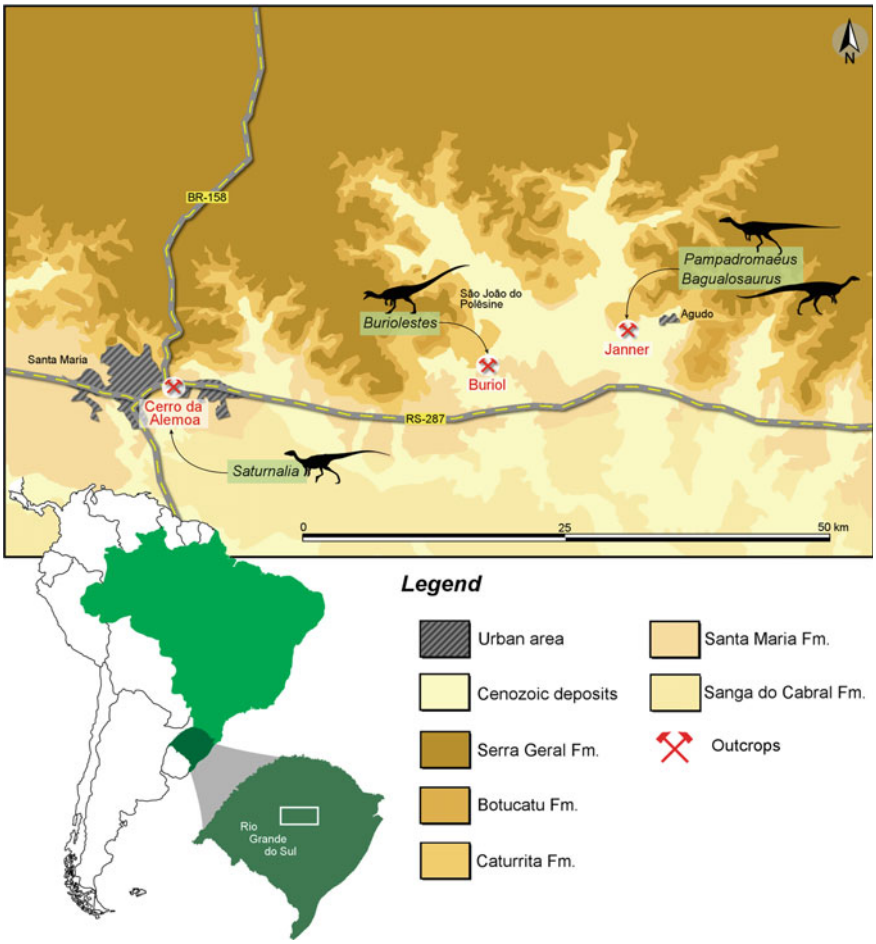

Fig. 3 Geological surface distribution map of the central part of Rio Grande do Sul, Brazil, indicating the sites where the specimens of *Saturnalia tupiniquim*, *Buriolestes schultzi*, *Pampadromaeus barberenai*, and *Bagualosaurus agudoensis* were found

rock samples were radioisotopically dated as 233.23 ± 0.73 Ma (Langer et al. 2018). The entire mudstone package at 'Cerro da Alemoa' corresponds to the upper portions of the Alemoa Member in the area (Da Rosa 2015), which in turn belong to the lower part of the Candelária Sequence, within the Santa Maria Supersequence (Horn et al. 2018; Schultz et al. 2020). In biostratigraphic terms, the fauna of the site fits the *Hyperodapedon* Acme-Zone (Langer et al. 2007), within the eponymous Assemblage-Zone (Schultz et al. 2020).

Proposed Phylogenetic Relations Because it was the first Carnian sauropodomorph recognised as such, at a time when *E. lunensis* was not assigned to the group, *Sat. tupiniquim* was depicted as sister to all other sauropodomorphs in the first phylogenetic studies dealing with it (Langer et al. 1999; Yates 2003, 2004, 2017a, b; Yates and Kitching 2003; Langer 2004; Pol 2004; Langer and Benton 2006; Ezcurra 2006; Sereno 2007a; Ezcurra and Novas 2007; Upchurch et al. 2007; Irmis et al. 2007; Martínez 2009; Nesbitt et al. 2009; but see Galton and Upchurch 2004; Barrett et al. 2007). With the description of other Carnian members of the group, the position of *Sat. tupiniquim* shifted among phylogenetic proposals, although most frequently forming a minimal clade with *Ch. novasi* (Ezcurra 2010; Novas et al. 2011; Apaldetti et al. 2011; Martínez et al. 2012b; Otero and Pol 2013; McPhee et al. 2014, 2015; Otero et al. 2015; Müller et al. 2016a, b, 2017b, 2018a; Cabreira et al. 2016; Cerda et al. 2017; Wang et al. 2017; Bronzati et al. 2018, 2019a; Bronzati and Rauhut 2018; Zhang et al. 2018; McPhee and Choiniere 2018; Marsola et al. 2018; Chapelle and Choiniere 2018; Marsh and Rowe 2018; Chapelle et al. 2019; McPhee et al. 2018, 2020; Langer et al. 2019; Garcia et al. 2019; Pacheco et al. 2019; Pretto et al. 2019; Pol et al. 2021). When all non-bagualosaur sauropodomorphs are joined in a clade (e.g. Ezcurra 2010; Novas et al. 2011; Martínez et al. 2011; Langer et al. 2017), *Sat. tupiniquim* is sometimes allied (apart from *Ch. novasi*) with *Pan. protos* and/or *Pam. barberenai* (Baron et al. 2017a; Müller et al. 2018a; McPhee et al. 2020). When early sauropodomorph phylogeny is arranged in a more pectinate fashion, *Sat. tupiniquim* most frequently nests closer to bagualosaurs than to other Carnian forms (Martínez and Alcober 2009; Alcober and Martínez 2010; Cabreira et al. 2011, 2016; Martínez et al. 2012b; Bittencourt et al. 2015; McPhee et al. 2015; Müller et al. 2016a, b, 2017a, b, 2018a; Wang et al. 2017; Agnolín and Rozadilla 2018; Pretto et al. 2017; Bronzati et al. 2017, 2018, 2019a; Zhang et al. 2018; Marsola et al. 2018; Bronzati and Rauhut 2018; Dal Sasso et al. 2018; Garcia et al. 2019; Pacheco et al. 2019; but see Cabreira et al. 2011; Baron and Barrett 2017; Baron et al. 2017b; Parry et al. 2017; Chapelle and Choiniere 2018; 2018b; Chapelle et al. 2019; Pretto et al. 2019; Pol et al. 2021), notably *E. lunensis* and/or *Bu. schultzi* (Marsh and Rowe 2018; McPhee and Choiniere 2018; Cau 2018; Baron and Williams 2018; McPhee et al. 2018; Marsh et al. 2019), sometimes forming a clade with *Ch. novasi* and other taxa (2018c; Langer et al. 2019; Müller 2020). One investigative analysis of Pretto et al. (2019) was the only so far not to find *Sat. tupiniquim* as a sauropodomorph, but instead forming a Guaibasauridae clade outside Eusaurischia. More recently, Müller and Garcia (2020) found *Sat. tupiniquim* forming, together with *Nh. waldsangae*, *Ba. agudoensis*, and *Ch. novasi*, the sister clade (= Saturnaliidae) to post-Carnian

sauropodomorphs, within which Garcia et al. (2021) found a sister taxon relation between *Sat. tupiniquim* and *Nh. waldsangae*.

General Anatomy and Paleobiology The sacral and pelvic (girdle and limb) anatomy and scapular skeleton of *Sat. tupiniquim* were respectively described by Langer (2003) and Langer et al. (2007). Later, a series of studies described the cranial (Bronzati et al. 2019a) and endocranial (Bronzati et al. 2017, 2019b) anatomy of this taxon. Femoral circumference allowed estimating its body mass in about 6.5 to 11 kg (Delcourt et al. 2012; Benson et al. 2014), showing that *Sat. tupiniquim* was a light-weighted, gracile dinosaur. Its neck is as long as ca. 0.6 of the trunk, which is slightly above the length seen in other early dinosaurs like *E. lunensis* (Bronzati et al. 2017). Hence, although the femur and tibia of all specimens are subequal in length (ca. 15 cm) to those of the *E. lunensis* holotype, *Sat. tupiniquim* was most probably somewhat longer, reaching about 1.5 *m* in length. Its hindlimbs are about 1.5 times longer than the forelimbs, and comparisons between its humeral and femoral circumferences, as well as the position of the humerus in relation to the shoulder girdle, indicate that *Sat. tupiniquim* was most likely a bipedal animal (Delcourt et al. 2012; McPhee et al. 2018). Yet, humeral traits as the large deltopectoral crest and expanded distal articulation suggest that *Sat. tupiniquim* was somehow intermediary, in terms of employing the forelimb for locomotion, between the condition seen in coeval dinosaurs, such as *E. lunensis*, and their Norian relatives (Langer et al. 2007).

The skull length of MCP 3845 was estimated at less than 10 cm, based on the lengths of the frontals and dentaries. This is about two-thirds the femoral length, as seen in younger sauropodomorphs, and unlike all other Carnian members of the group, except for *Ba. agudoensis*, for which skull and femora are known (i.e. *Bu. schultzi*, *E. lunensis*, *Pam. barberenai*, and *Pan. protos*; Bronzati et al. 2017, 2019a). The teeth of *Sat. tupiniquim* have small serrations, and some are gently curved distally, fitting better a faunivorous diet. Some studies suggested that it was either an herbivore (Langer et al. 1999) or an omnivore (Barrett and Upchurch 2007), but the lack of both coarse denticles and overlap between adjacent crowns contradicts this inference. On the other hand, the brain of *Sat. tupiniquim* exhibits a relatively large cerebellar flocculus, a structure related to the control of head and neck movements and it is also involved in gaze stabilisation. Predatory birds generally have larger flocculi in relation to their non-predatory relatives (Ferreira-Cardoso et al. 2017). In this sense, the large cerebellar flocculus of *Sat. tupiniquim* could potentially be related to a feeding habit involving the capture of small and elusive prey (Bronzati et al. 2017).

Panphagia protos Martínez and Alcober 2009

Holotype The holotype and only known specimen of *Pan. protos* (PVSJ 874) corresponds to a skeletally immature individual represented by a partial skull and postcranium (Martínez and Alcober 2009; Table 1).

Geographic and Stratigraphic Provenance The holotype of *Pan. protos* was found at the Valle Pintado locality, Hoyada de Ischigualasto, Ischigualasto Provincial Park, San Juan, Argentina (Fig. 2). It came from the lower levels of the Cancha de

Bochas Member, 40 m above the base of the unit (*Hyperodapedon-Exaeretodon-Herrerasaurus* biozone), near the beds dated in 231.4 ± 0.3 Ma (Martínez and Alcober 2009; Martínez et al. 2012b; Colombi et al. 2021).

Proposed Phylogenetic Relations *Panphagia protos* was originally recovered as the earliest branching member of Sauropodomorpha (Martínez and Alcober 2009), and this position was also found in some subsequent studies (e.g. Alcober and Martínez 2010; Martínez et al. 2012b). Other phylogenetic analyses have recovered *Pan. protos* within Saturnaliidae (e.g. Ezcurra 2010; Martínez et al. 2011; Novas et al. 2011; Müller et al. 2018a, b; Langer et al. 2019) or as one of the sister taxa to the Saturnaliidae + Bagualosauria clade (e.g. Pacheco et al. 2019). Müller and Garcia (2020) found *Pan. protos* forming a clade with *Pam. barberenai* sister to a Bagualosauria including *Sat. tupiniquim* and *Ch. novasi*. Pol et al. (2021) found *Pan. protos*, along with *Bu. schultzi*, as one of the earliest branching sauropodomorphs. Beyond these alternative positions, the non-bagualosaur sauropodomorph affinities of *Pan. protos* have been stable among the published phylogenetic analyses.

General Anatomy and Paleobiology The general anatomy of *Pan. protos* has been described by Martínez and Alcober (2009), whereas its cranial elements were described in more detail by Martínez et al. (2012c). The tibia of PVSJ 874 is subequal in length to those of *E. lunensis* and *Sat. tupiniquim* (i.e. ca. 15 cm), matching the total skeletal length reconstructed as 1.3 m by Martínez and Alcober (2009). The preserved lower jaw indicates that *Pan. protos* has a relatively long skull, as in *E. lunensis* and proportionally longer than those of *Sat. tupiniquim* and bagualosaurs (Martínez and Alcober 2009). The floccular fossa of the prootic and supraoccipital is proportionally large, as those of several other Carnian dinosauriforms (e.g. *Lewisuchus admixtus*: Ezcurra et al. 2020b; *Sat. tupiniquim*: Bronzati et al. 2017; *Gnathovorax cabreirai*: Pacheco et al. 2019; *Bu. schultzi*:2020), indicating enhanced gaze stabilisation and coordination of eye, head, and neck movements (Bronzati et al. 2017). The dentary tooth crowns are somewhat expanded at the base, with labial and lingual eminences, and relatively small and obliquely set denticles on the mesial and distal margins. This dental morphology has been interpreted as evidence of an omnivorous diet (Martínez and Alcober 2009). The cervical vertebrae are moderately elongated, similar to those of other Carnian sauropodomorphs. The scapula has a fan-shaped blade. The ilium has a partially opened acetabulum and the ischium has a conspicuously craniocaudally expanded distal end. The tibia has a sub-squared distal end, with an extensive facet for reception of the ascending process of the astragalus. The astragalus is similar to that of other early saurischians in the presence of a cranially prominent craniomedial corner of the body and a transversely reduced fibular facet.

Chromogisaurus novasi Ezcurra 2010

Holotype The holotype and only known specimen of *Ch. novasi* (PVSJ 845) corresponds to the partial skeleton of a probable adult individual (Table 1), but some of its elements have been subject to different interpretations. For example, the proximal end of the right ulna described by Ezcurra (2010) was alternatively interpreted as

the caudal end of a rhynchosaur right hemimandible (Martínez et al. 2012b). Also, a partial metatarsal II was assigned either to the left (Ezcurra 2010) or to the right (Martínez et al. 2012b) side, and articulated phalanges were assigned to the left pedal digit II by Ezcurra (2010) and to the right pedal digit III by Martínez et al. (2012b).

Geographic and Stratigraphic Provenance The holotype of *Ch. novasi* was collected at the Valle Pintado locality, Hoyada de Ischigualasto, Ischigualasto Provincial Park, San Juan, Argentina (Fig. 2). PVSJ 845 was found in the lower levels of the Cancha de Bochas Member, 40 m above the base of the unit (*Hyperodapedon-Exaeretodon-Herrerasaurus* biozone), at about the same level dated in 231.4 ± 0.3 Ma (Ezcurra 2010; Martínez et al. 2012a; Colombi et al. 2021).

Proposed Phylogenetic Relations In the phylogenetic analysis that accompanied its first description, *Ch. novasi* was recovered as the sister taxon of *Sat. tupiniquim*, forming a clade of early sauropodomorphs now recognised as Saturnaliidae (Ezcurra 2010). All subsequent analyses found a sister taxon relationship between *Ch. novasi* and *Sat. tupiniquim* among non-bagualosaur sauropodomorphs (e.g. Novas et al. 2011; Martínez et al. 2012b; Cabreira et al. 2016; Langer et al. 2019; Pacheco et al. 2019; Pol et al. 2021). More recently, Müller and Garcia (2020) found *Ch. novasi* forming, together with *Sat. tupiniquim Nh. waldsangae*, and *Ba. agudoensis*, the sister clade (=Saturnaliidae) to post-Carnian sauropodomorphs.

General Anatomy and Paleobiology The holotype of *Ch. novasi* was described in detail by both Ezcurra (2010) and Martínez et al. (2012b). It corresponds to a small-sized dinosaur with relatively gracile hindlimbs. Yet, its ca. 17.5 cm long tibia suggests that it was somewhat larger than *E. lunensis*, *Sat. tupiniquim*, and *Pan. protos*, likely surpassing 1.5 m in total body length. Unfortunately, the specimen lacks cranial bones and this precludes assessing several aspects of its palaeobiology. The presence of closed neurocentral sutures in the caudal vertebrae and fusion between the scapula and coracoid indicates that the holotype was probably a skeletally mature individual (Ezcurra 2010; Martínez et al. 2012b). The only possible preserved forelimb bone is the proximal end of the right ulna (Ezcurra 2010), which was also interpreted as a partial rhynchosaur hemimandible (Martínez et al. 2012b). Yet, the glenoid region of a rhynchosaur hemimandible (e.g. *Hyperodapedon sanjuanensis*; MACN-Pv 18,185) differs from this element in the presence of a transversely broad ventral surface, with a distinct longitudinal change of slope on the lateral surface of the surangular; an upturned caudal end of the articular; a transversely broader glenoid fossa; and a smooth lateral surface of the hemimandible. By contrast, the bone of PVSJ 845 closely resembles the proximal end of the ulna of *Sat. tupiniquim*, including the presence of a long olecranon process and a strongly striated lateral surface of the bone, and may indeed represent a right ulna (MDE pers. obs.). The size of the olecranon process and its striated surface indicate an extensive insertion area for the *M. triceps* and probably strong forearm extension. The ilium has a partially closed acetabular wall and a relatively long postacetabular process. The preserved femora are incomplete, but their length was probably subequal to that of the tibia. The tibia has a long and laterally curved cnemial crest, and the distal end is sub-squared, with

an extensive facet for reception of the ascending process of the astragalus. Metatarsal II is the only preserved metatarsal, but interpreted as from either the left (Ezcurra 2010) or the right (Martínez et al. 2012b) side. Although the profile of the distal end of the bone resembles that of the right metatarsal II of other early dinosaurs (Martínez et al. 2012b), the curvature of the shaft would result in an unusual bowing towards metatarsal III and not inwards. Thus, although there is conflicting evidence for the interpretation of this bone, the bowing of the shaft favours the interpretation as a left side element (MDE pers. obs.). Similarly, the articulated pedal digit was interpreted as either a left digit II (Ezcurra 2010) or a right digit III (Martínez et al. 2012b). This digit has two non-ungual and one ungual phalanges; thus, it would be complete if interpreted as a digit II but would lack its proximal most phalanx if interpreted as digit III. The proximal articular surface of the most proximally preserved phalanx is continuously concave, indicating that it is articulated with a metatarsal. By contrast, if it articulated with a missing proximal phalanx, it would have had a median vertical ridge for articulation with the ginglymus of that phalanx. Thus, it seems more likely that this digit represents a complete left digit II (MDE pers. obs.).

Pampadromaeus barberenai Cabreira, Schultz, Bittencourt, Soares, Fortier, Roberto da Silva and Langer 2011

Holotype The holotype of *Pam. barberenai* (ULBRA-PVT016) corresponds to a partial skeleton (Table 1), with most elements preserved disarticulated over an area of less than half square metres, within a single block of sediment. Few other bones assigned to the holotype were collected from around that block. The assignment of these elements to a single individual is possible due to the lack of duplicated parts, similar taphonomic signatures, and matching morphology and size.

Reffered Specimens and Discoveries Specimens referred to *Pam. barberenai* include two fairly complete and isolated left femora: CAPPA/UFSM 0027 (2015) and 0028 (2017a).

Geographic and Stratigraphic Provenance The holotype and both referred specimens of *Pam. barberenai* were collected in the site known as 'Sítio Janner' or 'Várzea do Agudo' (Fig. 3; Cabreira et al. 2011; 2015, 2017a; Da Rosa 2015; Pretto et al. 2015, 2019) that is located about two kilometres to the west of the town of Agudo (coordinates: 53° 17′ 34.20″ W, 29° 39′ 10.89″ S). In the site, fossils are concentrated in the upper half of the massive to laminate, red mudstones interpreted to have accumulated in a distal floodplain palaeoenvironment, overlaid in erosive contact by a light-coloured, cross-bedded sandstone that represents a river channel (Pretto et al. 2015; Da Rosa 2015). The holotype (ULBRA-PVT-016) was collected at the base of the fossiliferous layer, about eight metres below the sandstone (Pretto et al. 2015), which also yielded the two referred femora (2017a). The mudstones at 'Sítio Janner' correspond to the upper portions of the Alemoa Member in the area (Zerfass 2007; Da Rosa 2015; Godoy et al. 2018), which in turn belongs to the lower part of the Candelária Sequence, Santa Maria Supersequence (Horn et al. 2018; Schultz et al. 2020). In biostratigraphic terms, the record of *Hyperodapedon* places the site in the eponymous Assemblage Zone (Schultz et al. 2020). However, rhynchosaurs

are scarce in the site, which is dominated by the cynodont *Exaeretodon*, suggesting a placement above the *Hyperodapedon* Acme-Zone of Langer et al. (2007). Thus, the dinosaur-bearing beds of 'Sítio Janner' are probably slightly younger than those of 'Cerro da Alemoa', dated as 233.23 ± 0.73 Ma (Langer et al. 2018).

Proposed Phylogenetic Relations *Pampadromaeus barberenai* was first considered as an early diverging sauropodomorph, with variable positions depending on the phylogenetic dataset employed by Cabreira et al. (2011): i.e. closer to *Pan. protos*, in a polytomy with *Sat. tupiniquim* + *Ch. novasi*, *Gu. candelariensis* and bagualosaurs (Ezcurra 2010); forming a polytomy with *Sat. tupiniquim*, *Pan. protos*, and bagualosaurs (Martinez and Alcober 2009); sister taxon to the clade formed by *Sat. tupiniquim* + bagualosaurs (Nesbitt et al. 2010); forming a clade with bagualosaurs, which is sister to the clade formed by *E. lunensis*, *Pan. protos*, and *Sat. tupiniquim* (Martínez et al. 2011). A similarly floating positioning was also found by other subsequent phylogenetic studies. When Saturnaliidae is recovered, *Pam. barberenai* can be found both as one of the early diverging members of the clade (Langer et al. 2017, 2019; 2018c; Müller 2020) or more deeply nested, close to *Sat. tupiniquim* (Baron et al. 2017a; Dal Sasso et al. 2018; Müller et al. 2018a; Pretto et al. 2019). Alternatively, *Pam. barberenai* is also found outside Saturnaliidae, as sister to the clade formed by that group and bagualosaurs (Martínez et al. 2012b, 2015; Pretto et al. 2019; Müller and Garcia 2020), which frequently also includes *Pan. protos* in a polytomy (Cabreira et al. 2016; Müller et al. 2017b, 2018a; Baron and Williams 2018; Garcia et al. 2019; Marsola et al. 2018). Other hypotheses place *Pam. barberenai* as sister to the clade formed by Guaibasauridae and post-Carnian sauropodomorphs (Baron and Barrett 2017; Parry et al. 2017; 2018b), sister to post-Carnian sauropodomorphs (Baron and Williams 2018), or even to all other sauropodomorphs (2017a). Besides, the taxon sometimes forms a minimal clade with either *Pan. protos* (Müller et al. 2018a; Bronzati et al. 2019a; Pacheco et al. 2019; Müller and Garcia 2020) or *Bu. schultzi* (Pretto et al. 2019).

General Anatomy and Paleobiology The holotype of *Pam. barberenai* was described in a preliminary fashion by Cabreira et al. (2011), and more comprehensively by Langer et al. (2019). Its humerus and femur have been reconstructed from fairly complete bones to ca. 8.5 and 14 cm long, respectively, and a complete fibula is 15 cm long. These measurements broadly match those of *E. lunensis*, suggesting a body length somewhat below 1.5 *m*, and its partially fused sacral zygapophyses suggest that ULBRA-PVT-016 was reaching osteological maturity. The skull of *Pam. barberenai* is plesiomorphicaly long, compared to the shorter skulls of *Sat. tupiniquim* and bagualosaurs. The pectoral limb is characterised by a transversely expanded distal end of the humerus and a long ulna with a relatively short olecranon process (although the association of this bone to the holotype is not beyond uncertainty). The iliac acetabulum is semi-perforated, and the pelvic epipodium is significantly longer than the femur, although this could be the result of proximodistal compression of the femora. Recent optimisations of early dinosaurs feeding behaviour have suggested faunivory as the ancestral sauropodomorph condition, including *Pam. barberenai* (Cabreira et al. 2016). However, most of its teeth are

lanceolate with coarse denticles along the carinae, more closely resembling those of bagualosaurs than those of other Carnian forms such as *Sat. tupniquim*, *E. lunensis*, and *Bu. schultzi*. This dental pattern is more broadly accepted as related to an omnivorous diet, rather than with pure faunivory. One of the isolated femora referred to *Pam. barberenai* (CAPPA/ UFSM 0028) is about 80% the length of the other, corresponding to an animal also relatively smaller that the holotype (2017a). It bears some traces related to osteological immaturity, probably representing a juvenile individual.

Buriolestes schultzi Cabreira, Kellner, Dias-da-Silva, Roberto da Silva, Bronzati, Marsola, Müller, Bittencourt, Batista, Raugust, Carrilho, Brodt and Langer 2016

Holotype The holotype of *Bu. schultzi* (ULBRA-PVT280) is composed of a partial skull (lacking most of the roof, palate, and braincase), complete lower jaw, and partial postcranial skeleton (Table 1; Cabreira et al. 2016).

Reffered Specimens Müller et al. (2017b, 2018a) referred further specimens to *Bu. schultzi* (Table 1), the most complete of which (CAPPA/UFSM 0035) preserves the entire skull and a partial postcranial skeleton, lacking forearm, manus, and tail. Other, less complete specimens referable to *Bu. schultzi* include a partial axis (CAPPA/UFSM 0179) and a complete right femur (ULBRA-PVT289). Müller et al. (2018a) also assigned the slightly more complete ULBRA-PVT056—preserving some neck vertebrae, a partial pelvic girdle, a right femur, and pedal phalanges—to *Bu. schultzi*. This corresponds to a significantly smaller specimen, about 2/3 the linear size of the holotype, which may indeed represent a less mature individual (Müller et al. 2018a). In fact, some of its notable anatomical differences relative to other specimens of *Bu. schultzi* can be explained by ontogeny, but a more comprehensive study of that specimen is needed to fully endorse that proposal.

Geographic and Stratigraphic Provenance All specimens mentioned in the previous section were collected in the site known as 'Buriol ravine' (Cabreira et al. 2016; Müller et al. 2018a), which is located about five kilometres south of São João do Polêsine (Fig. 3), in the eponymous municipality (coordinates: 29° 39′ 34.2″ S, 53° 25′ 47.4″ W). The site exposes the mudstones of the upper part of the Alemoa Member, Santa Maria Formation (Zerfass 2007; Godoy et al. 2018), which corresponds to the lower portion of the Candelária Sequence (Horn et al. 2018) of the Santa Maria Supersequence (Zerfass et al. 2003). The abundance of hyperodapedontine rhynchosaurs and absence of the cynodont *Exaeretodon* suggest that this site belongs to the *Hyperodapedon* Acme-Zone (Langer et al. 2007), within the eponymous Assemblage-Zone (Schultz et al. 2020). As such, it may have a similar age to the 'Cerro da Alemoa' site, which was radioisotopically dated as 233.23 ± 0.73 Ma (Langer et al. 2018).

Proposed Phylogenetic Relations In its original description, *Bu. schultzi* was placed as the sister taxon to all other sauropodomorphs (Cabreira et al. 2016). This hypothesis has been corroborated by following studies that employed modified versions of that dataset (Müller et al. 2017b, 2018a; Bronzati et al. 2019a; Garcia et al. 2019, 2021; Marsola et al. 2018; Pretto et al. 2019; Pacheco et al. 2019;

Müller and Garcia 2020), as well as different datasets (Cau 2018; 2018c; Baron and Williams 2018; Ezcurra et al. 2020a; Müller 2020). In the case of Pol et al. (2021), that position is shared in a polytomy by *P. protos*. Instead, other phylogenetic hypotheses, also showing a pectinate arrangement of early sauropodomorphs, found *E. lunensis* in such earliest branching position, with *Bu. schultzi* grouped with all other sauropodomorphs, either as their sister taxon (Bronzati et al. 2019a; Langer et al. 2019) or more highly nested (Pretto et al. 2019). Studies that found a clade of Carnian sauropodomorphs are mostly derived from the study of Langer et al. (2017). In these cases, *Bu. schultzi* is never the sister taxon of all other members of the clade, but more highly nested instead, although usually external to the clade formed by *Sat. tupiniquim* and *Pan. protos* and/or *Pam. barberenai* (Parry et al. 2017; Baron et al. 2017a; McPhee et al. 2020; Baron 2019; Garcia et al. 2019). Dal Sasso et al. (2018) and one of the investigative analyses of Pretto et al. (2019) were the only studies not to find *Bu. schultzi* as a sauropodomorph. Instead, the taxon was positioned, respectively, as a theropod closer to neotheropods and forming a Guaibasauridae clade of non-eusaurischian saurischians.

General Anatomy and Paleobiology The holotype of *Bu. schultzi* (ULBRA-PVT280) was described in a preliminary fashion by Cabreira et al. (2016), but CAPPA/UFSM 0035 was fully described by (Müller et al. 2018a) and the axis CAPPA/UFSM 0179 by Müller et al. (2017b). Together, ULBRA-PVT280 and CAPPA/UFSM 0035 reveal details of the almost entire skeleton of this dinosaur, lacking only parts of the tarsus and manus. They correspond to individuals of about the same size, with femora of ca. 13 cm of length. Compared to other coeval sauropodomorphs, this suggests a total body length slightly below that of *E. lunensis*, whereas the isolated axis CAPPA/UFSM 0179 reveals a larger individual and the possible sub adult ULBRA-PVT056 is below 1.0 m of total body length (Müller et al. 2018a). The general body plan of *Bu. schultzi* resembles that of other coeval sauropodomorphs, suggesting a fully bipedal posture. The skull is relatively long, the external nares are reduced, and the long rostrum is about half the skull length. There is a marked subnarial gap separating the alveolar margins of the premaxilla and maxilla, the former of which is downturned. The teeth are blade-like, distally recurved, with fine serrations that form right angles with the crown margins, a condition associated with a faunivorous feeding behaviour (Cabreira et al. 2016). The neck is about two-thirds of the trunk length and two vertebrae form the bulk of the sacral articulation. The humerus is gracile, lacking a strongly expanded distal end, and the ulna lacks a pronounced olecranon process. The acetalubum is almost fully closed and the tibia is longer than the femur. An almost complete cranial endocast was reconstructed from the skull of CAPPA/UFSM 0035 (Müller et al. 2020). It resembles that of *Sat. tupiniquim*, with a relatively large cerebellar flocculus (Bronzati et al. 2017). In adition, the *Bu. schultzi* endocast allowed the reconstruction of the entire forebrain, revealing olfactory bulbs significantly larger than those predicted for dinosaurs of similar body mass (Müller 2021). Therefore, in addition to advanced coordination of eye, head, and neck movements, *Bu. schultzi* would have had an enhanced sense of smell.

Bagualosaurus agudoensis Pretto, Langer and Schultz 2019

Holotype The holotype and only known specimen of *Ba. agudoensis* (UFRGS-PV-1099-T) comprises a partial skull associated with a partial postcranial skeleton, including some vertebrae, the pelvic girdle, and hindlimbs (Table 1; Pretto et al. 2019).

Geographic and Stratigraphic Provenance The holotype was unearthed from 'Sítio Janner' (see *Pam. barberenai* above; Fig. 3), about three metres below the sandstone layer that tops the outcrop (Pretto et al. 2019).

Proposed Phylogenetic Relations In the original description, *Ba. agudoensis* was found as the sister taxon to all other bagualosaurs (Pretto et al. 2019), a clade that circumscribes the entire diversity of unambiguous post-Carnian sauropodomorphs (Langer et al. 2019). Such an affinity was corroborated by most later analyses (Müller et al. 2018c; Bronzati et al. 2019a; Langer et al. 2019; Müller 2020; Pol et al. 2021), but Pacheco et al. (2019) found the taxon in a polytomy with other bagualosaurs. Müller and Garcia (2020) and Garcia et al. (2021) were so far the only studies to positively question the placement of *Ba. agudoensis* as the most immediate sister taxon to all post-Carnian bagualosaurs, suggesting instead that it forms a Carnian clade with only *Sat. tupiniquim*, *Ch. novasi*, and *Nh. waldsangae*.

General Anatomy and Paleobiology *Bagualosaurus agudoensis* is unique among Carnian sauropodomorphs for its relatively large size. It is about 2.5 m long, whereas coeval sauropodomorphs (see above) were animals of ca. 1.5 m. An estimation of its body mass, applying the Campione et al. (2014) equation to the femoral circumference of the holotype (= 83 mm) results in 40 kg. In addition, *Ba. agudoensis* shares with post-Carnian sauropodomorphs (and *Sat. tupiniquim*) a proportionally reduced head (Bronzati et al. 2019b; Pretto et al. 2019). The alveolar margin of the premaxilla and maxilla forms a straight line, unlike the ventrally sloped alveolar margin of the premaxilla of *Bu. schultzi*, *Pam. barberenai*, and *E. lunensis*. The teeth have large denticles, forming oblique angles to the crown margins (Pretto et al. 2019). The pelvic girdle and hind limb of *Ba. agudoensis* are plesiomorphic in comparison to those of younger bagualosaurs. The medial wall of the ilium is well developed ventrally, so that the acetabulum is not fully perforated; the femur is sigmoid, has a trochanteric shelf, and the fourth trochanter is within the proximal half of the bone. The foot is gracile, with elongated phalanges, when compared to most bagualosaurs. The jaw/tooth anatomy reveals a probably omnivorous animal, but more dependent on plant intake that other Carnian sauropodomorphs. The gracile hindlimb, with femur and epipodium of about the same length, indicates that *Ba. agudoensis* was most probably not an obligate quadruped.

4 Alpha-Taxonomy of the Carnian Sauropodomorphs

4.1 Uniqueness of the Holotypes

One of the questions raised about the alpha-taxonomy of the Carnian sauropodomorphs from South America is the possible synonymy between some of the named taxa. In order to tackle this question, we identify below a minimal set of anatomical traits that allow differentiating each of them from one another. Only after such a procedure, we can validate their inclusion as unique terminals in the phylogenetic analyses.

4.1.1 Eoraptor lunensis (PVSJ 512)

Sereno et al. (2012) provided a revised diagnosis of *E. lunensis* based on the following autapomorphies: dorsomedial ramus of the caudal process of premaxilla slender with tongue-shaped distal expansion; nasal with transversely broad, horizontal shelf with a convex lateral margin that overhangs the antorbital fossa; pterygoid process on caudal palate margin that articulates laterally in a synovial socket in the ectopterygoid; narrow premaxilla-maxilla diastema approximately one crown in width; maxillary crowns with a prominent lateral eminence; accessory articular process on the medial aspect of mid-cervical prezygapophyses; extreme hollowing of dorsal centra and neural arches. Yet, several of these features cannot be accessed in the holotypes of other Carnian sauropodomorphs, so further comparison is required to establish the uniqueness of PVSJ 512 and, henceforth, *E. lunensis*.

We concur with some of the traits used by Sereno et al. (2012) to differentiate PVSJ 512 from PVSJ 874 (holotype of *Pan. protos*), namely: a shallower lateral neurovascular groove on the dentary; a less pronounced ridge on the lateral aspect of the surangular; a less distally expanded scapular blade, with a distal margin broadly perpendicular to its long axis; a more elongate pubic blade (more than four times the distal width). In addition, we agree with some other differential traits of *E. lunensis*, relative to *Pan. protos*, mentioned by Martínez and Alcober (2009), i.e.: nasal with a more convex lateral margin and lacking an elongated rostral fossa; a transversally narrower lateral flange of the quadrate, with a smaller and more medially paced quadrate foramen; a straight caudal half of the ventral border of the dentary (rather than concave) in lateral view; maxillary and dentary 'cheek' tooth-crowns with concave distal margins; stouter (craniocaudally) mid-cranial neck vertebrae; pubic peduncle of the ilium with a sharp (rather than rounded) dorsal margin; cranially arched pubic shaft; ischium with a less expanded distal end and subtriangular (rather than rounded) mid-shaft section and distal outline.

Likewise, we endorse some traits identified by Ezcurra (2010), Sereno et al. (2012), and Martínez et al. (2012b), which differentiate PVSJ 512 from PVSJ 845 (holotype of *Ch. novasi*), namely: a non-hypertrophied olecranon process of the ulna; a more prominent iliac supra-acetabular crest; a more medially expanded femoral

head; a markedly asymmetrical fourth trochanter; a more transversely expanded distal end of the tibia (although its transverse compression may be a taphonomic artefact in *Ch. novasi*); a less concave distal margin of the tibia in medial view.

In addition to its distinction relative to the holotypes of *Pan. protos* and *Ch. novasi*, PVSJ 512 differs from MCP 3844-PV (holotype of *Sat. tupiniquim*) by a less concave caudal margin of the scapular blade, a less pointed (not 'hook-like') distal corner of the humeral deltopectoral crest, a less lateromedially expanded distal articulation of the humerus, a not enlarged olecranon process of the ulna, and a less dorsoventrally expanded distal end of the ischium. We also concur with Langer et al. (2018) that PVSJ 512 differs from ULBRA-PVT280 (holotype of *Pam. barberenai*) in that the premaxilla has a longer dorsomedial ramus of the caudal process, the base of the dorsal ramus of the maxilla lacks a large rostrally opening lateral foramen, the antorbital fossa is not excavated by a promaxillary fossa, the ventral margin of the antorbital fossa is marked by a rounded ridge, a web of bone spans rostroventrally from the junction between rostral and ventral rami of lacrimal, there is a raised lip forming the prearticular margin of the internal mandibular fenestra, there is a set of rostral foramina at the lateral surface of the dentary, the first premaxillary tooth bears denticles, the maxilla has less than 20 teeth, the maxillary and dentary 'cheek' tooth-crowns have concave distal margins, denticles set perpendicular to the tooth margins, and not restricted to their apical part, the pterygoid bears a transverse row of palatal teeth, the first dentary tooth is inset from the rostral margin of the bone, the scapular blade is short relative to its minimal craniomedial breadth, the dorsal margin of the acromion process forms a lower angle to the cranial margin of the scapular blade, the distal end of the humerus is less transversally expanded, the brevis shelf is connected to the supra-acetabular crest, and metatarsal IV has a broader than deep distal outline.

PVSJ 512 also differs from ULBRA-PVT280 (holotype of *Bu. schultzi*) in that the preorbital region of the skull is shorter, the dorsomedial ramus of the caudal premaxillary process is longer, the maxilla-premaxilla contact bears a subnarial foramen, the forked part of the caudal ramus of the jugal is more rostrally located along the ventral margin of the lower temporal fenestra, the deltopectoral crest of the humerus is proximodistally longer, and the pubic pair lacks a bevel on its distal margin. Finally, PVSJ 512 differs from UFRGS-PV-1099-T (holotype of *Ba. agudoensis*) for its much smaller size, proportionally longer head, first tooth not inset from the rostral margin of the premaxilla, concave ventral margin of the premaxilla-maxilla contact, more ventrally placed subnarial foramen, maxillary and dentary 'cheek' tooth crowns with concave distal margins and smaller denticles along the carinae, and distal end of the tibia lacking a caudomedial notch.

4.1.2 Saturnalia tupiniquim (MCP 3844-PV)

Langer et al. (2007) provided the last emended diagnosis of *Sat. tupiniquim*, but this was based only on the pectoral skeleton and elaborated when no other Carnian sauropodomorph, except for *E. lunensis* (not assigned to the group at the time), was

known. As such, it obviously fails to differentiate *Sat. tupiniquim* from more recently described taxa, and this is attempted below.

In addition to the differences relative to the holotype of *E. lunensis* (provided in the previous section), MCP 3844-PV differs from PVSJ 874 (holotype of *Pan. protos*) based on—partially as reviewed by Martínez and Alcober (2009)—a markedly concave caudal margin of the scapular blade, an ilium with an incipient postacetabular embayment and a concave (rather than straight, in dorsal view) caudal margin of the postacetabular ala, a subtriangular (rather than hemispherical) mid-shaft section and distal outline of the ischium, a more cranially placed lateral condyle of the tibial proximal articulation, and a triangular (rather than parallelogram shaped) outline of the proximal end of metatarsal III. Likewise, we concur with Ezcurra (2010) and Martínez et al. (2012b) that MCP 3844-PV differs from PVSJ 845 (holotype of *Ch. novasi*) by an ilium with a less dorsoventrally extensive blade, a more expanded supra-acetabular crest, and a straighter ventral margin of the acetabular wall, a larger fibular condyle of the femur, a more cranially located lateral condyle of the tibia, a cnemial crest more cranially expanded close to the proximal margin of the tibia, and a not ventrally expanded lateral condyle of the distal end of metatarsal II.

Partially as reviewed by Langer et al. (2018), MCP 3844-PV differs from ULBRA-PVT016 (holotype of *Pam. barberenai*) based on a more concave caudal margin of the scapular blade, a greatly enlarged olecranon process of the ulna, the incorporation of a caudal vertebra to the sacrum, a supra-acetabular crest that reaches the distal end of the pubic peduncle, a straighter ventral margin of the iliac acetabular wall, a not hypertrophied fibular condyle of the femur, and a lateromedially broader metatarsal I distal articulation. MCP 3844-PV also differs from ULBRA-PVT280 (holotype of *Bu. schultzi*) by a longer deltopectoral crest of the humerus, with a hook-like distal corner, a lateromedially broader distal articulation of the humerus, a marked fossa olecrani on the caudal surface of the distal end of the humerus, a greatly enlarged olecranon process of the ulna, a distal end of the ischium more caudodorsally expanded and with a triangular distal outline, a cranially convex distal femur outline, and no caudal knob medial to the intercondylar notch of the tibia. Finally, MCP 3844-PV differ from UFRGS-PV-1099-T (holotype of *Ba. agudoensis*) by its overall smaller body size, as well as by a more ventrally expanded brevis shelf in the caudal end of the postacetabular ala, the lack of a groove excavating the ambiens process of the pubis, a 'semi-pendant' fourth trochanter on the femur, and tibia lacking a caudomedial notch in the distal end.

4.1.3 Panphagia protos (PVSJ 874)

Martínez and Alcober (2009) proposed that the holotype of *Pan. protos* differs from the only other Carnian sauropodomorphs known at the time (i.e. *E. lunensis* and *Sat. tupiniquim*) by the presence of a rostrocaudally elongated fossa on the base of the rostroventral process of the nasal, a wide lateral flange on the quadrate, with a large foramen located far from the shaft, a deep groove on the lateral surface of the lower jaw surrounded by prominent dorsal and ventral ridges, extending from

the position of ninth tooth to the surangular foramen, a caudoventral process of the dentary bifurcated in two slender rami that overlap the lateral surface of the angular, a long retroarticular process of the articular transversely wider than the articular area for the quadrate, an oval scar on the lateral surface of the caudal border of the cervical centra, distinct prominences located caudodorsally to the diapophyses on the neural arch of the cranial cervical vertebra, a dorsal end of the scapular blade nearly three times wider than the neck, a scapular blade with an expanded caudodistal corner limited by a wedged caudal border, and a medial lamina of brevis fossa twice wider than the iliac spine. Yet, not all of these features are preserved in PVSJ 512 and/or MCP 3844-PV, so that this differential diagnosis should be cross-checked with those given above for *Sat. tupiniquim* and *E. lunensis.*

In addition, PVSJ 874 differs from PVSJ 845 (holotype of *Ch. novasi*)—partially as reviewed by Martínez et al. (2012b)—by proximal tail vertebrae with less transversely compressed centra and leaf-shaped (rather than subtriangular) transverse processes, ilium with a transversely broader caudomedial shelf, a supra-acetabular crest not reaching the distal end of the pubic peduncle, a less concave ventral margin of the iliac acetabuluar wall, and a more prominent antitrochanter, and tibia with cnemial crest more cranially expanded closer to the proximal margin of the bone.

Partially as reviewed by Langer et al. (2018), PVSJ 874 differs from ULBRA-PVT016 (holotype of *Pam. barberenai*) in that the quadrate foramen is larger, the first dentary tooth is inset from the rostral margin of the bone, maxillary and dentary 'cheek' tooth crowns have smaller denticles, the scapular blade is shorter relative to its minimal craniocaudal breadth, forms a lower angle to the acromion process, and is more craniocaudally expanded towards its dorsal end, the pubic peduncle of the ilium has a rounded dorsal margin, and the caudal end of the brevis shelf is not so ventrally projected. PVSJ 874 also differs from ULBRA-PVT280 (holotype of *Bu. schultzi*) by tooth serrations forming oblique (rather than right) angles to the crown margin, less dorsoventrally expanded iliac lamina and preacetabular ala, a transversely broader caudal end of the postacetabular area (=brevis plus 'caudomedial' shelves), a pubis lacking a bevel on its distal margin, and a proximal articulation of the tibia that lacks a caudal knob, medial to the intercondylar notch. Finally, PVSJ 874 differs from UFRGS-PV-1099-T (holotype of *Ba. agudoensis*) in its smaller body size, proportionally longer head, and distal end of the tibia lacking a caudomedial notch.

4.1.4 Chromogisaurus novasi (PVSJ 845)

Martínez et al. (2012b) diagnosed *Ch. novasi* by the general combination of an ilium with a marked caudal projection of the postacetabular ala, an incipient perforation of the acetabular wall, and a supra-acetabular crest with a strongly concave acetabular surface, but not well projected laterally, a reduced fibular condyle in the femur, a medial surface of the proximal end of the fibula with an elongate rugosity adjacent to the cranial margin of the shaft, and metatarsal II with strongly dorsoventrally asymmetric distal condyles (the latter two traits considered autapomorphic). In addition to the differences relative to the holotypes of *E. lunensis*, *Sat. tupiniquim*, and *Pan.*

protos (provided in the previous sections), more specific comparisons for PVSJ 845 are given below.

Partially as reviewed by Langer et al. (2018), PVSJ 845 differs from ULBRA-PVT016 (holotype of *Pam. barberenai*) by an enlarged olecranon process of the ulna, a supra-acetabular crest of the ilium that reaches the distal end of the pubic peduncle, a femur with a symmetrical fourth trochanter and a not hypertrophied fibular condyle, and a fibula that bears a rugose cranial ridge on the medial surface of its proximal end and lacks a more distal rugose iliofibularis muscle insertion. It also differs from ULBRA-PVT280 (holotype of *Bu. schultzi*) in that the ulna has an expanded olecranon process, the ilium has a concave ventral margin of the acetabular wall and a more caudally facing distal facet of the ischial peduncle, the femur has a symmetrical fourth trochanter and a smaller fibular condyle, the distal end of the tibia is lateromedially compressed, and the fibula lacks a rugose *M. iliofibularis* insertion. Finally, PVSJ 845 differs from UFRGS-PV-1099-T (holotype of *Ba. agudoensis*) in its smaller body size, concave ventral margin of the iliac acetabular wall, and tibia with a well-developed fibular crest and lacking a caudomedial notch in the distal end.

4.1.5 Pampadromaeus barberenai (ULBRA-PVT016)

Langer et al. (2019) differentiated *Pam. barberenai* from other Carnian sauropodomorphs by the unique combination of partially fused zygapophyses in the primordial sacral pair, ulna longer than 80 per cent the humeral length, intercondylar groove of the femur broader lateromedially than the lateral and medial condyles, and metatarsal I with an L-shaped proximal outline, including a lateral expansion that covers part of the cranial surface of metatarsal II. Also, in addition to the differences relative to the holotypes of *E. lunensis*, *Sat. tupiniquim*, *Pan. protos*, and *Ch. novasi* (provided in the previous sections), more specific comparisons for ULBRA-PVT016 are given below.

Partially as reviewed by Langer et al. (2018), ULBRA-PVT016 differs from ULBRA-PVT 280 (holotype of *Bu. schultzi*) in that the premaxilla lacks a second foramen above the premaxillary foramen and has a not downturned ventromedial ramus of the caudal process, the first maxillary tooth is directed strictly ventrally, a promaxillary fossa is seen within the antorbital fossa, the forked portion of the caudal ramus of the jugal reaches base of the dorsal ramus, maxillary and dentary 'cheek' tooth crowns have sigmoid distal margins with large denticles set oblique to their margins, the second primordial sacral vertebra has a dorsally (rather than dorsocaudally) directed neural spine, the distal end of the humerus is transversely broader, the supra-acetabular crest is less laterally expanded, the pubic peduncle of the ilium has a sharp dorsal margin, and the femoral head has a less expanded medial tubercle. Also, ULBRA-PVT016 differs from UFRGS-PV-1099-T (holotype of *Ba. agudoensis*) for its smaller size, proportionally longer head, premaxillary and dentary with the first tooth not retreated, a premaxilla/maxilla contact lacking a subnarial foramen and a straight buccal margin, an antorbital fossa that does not reach the caudal portion of

the maxilla, a more slender dentary lacking a ventrally sloped rostral tip, a more concave acetabular roof, and an epipodium longer that the femur.

4.1.6 Buriolestes schultzi (ULBRA-PVT280)

ULBRA-PVT280 can be differentiated from the holotypes of *E. lunensis*, *Sat. tupiniquim*, *Pan. protos*, *Ch. novasi*, and *Pam. barberenai* based on the comparisons provided in the previous sections. Some of such futures were highlighted by Müller et al. (2018a), who listed a general combination of traits unique to *Bu. schultzi* among coeval sauropodomorphs, namely: skull slightly shorter than the femur; short dorsomedial ramus of the caudal premaxillary process; no premaxillary fossa on the medial maxillary wall; marked subnarial gap; forking part of the caudal process of the jugal projected from a pedicel; zyphodont dentition; craniocaudally short, raised rugose process on the dorsocaudal margin of the iliac blade; marked protuberance between the craniomedial crest and the dorsolateral trochanter of the femur; ovoid striated tuberosity on the craniomedial margin of the proximal third of the fibula. In addition to that, ULBRA-PVT280 differs from UFRGS-PV-1099-T (holotype of *Ba. agudoensis*) in its smaller body size, proportionally longer head, a premaxilla/maxilla contact lacking a subnarial foramen and a straight buccal margin, maxillary and dentary 'cheek' tooth crowns distally concave and with smaller denticles forming right angles to the tooth margin, epipodium slightly longer than the femur, and distal end of the tibia lacking a caudomedial notch.

4.1.7 Bagualosaurus agudoensis (UFRGS-PV-1099-T)

As revised above, if not only for its significantly larger size, UFRGS-PV-1099-T also differs from the holotypes of all the other Carnian sauropodomorphs from South America based on the series of traits previously mentioned for these taxa. Also, Pretto et al. (2019) diagnosed the taxon based on a short skull, less than two-thirds of femoral length, premaxillary and dentary teeth retracted from the rostral margin of the bones, first premaxillary tooth at least as high as the highest maxillary tooth, no subnarial gap or diastema, most teeth lanceolate with coarse serrations along the carinae, straight ventral margin of iliac acetabulat wall, straight dorsal surface of the iliac acetabulum, lateromedially widened pubic peduncle, with no dorsal crest, pubic tubercle with a distinct longitudinal sulcus, femoral subequal in length to tibia and/or fibula, tibia lacking a marked fibular crest and with a conspicuous caudomedial notch in the distal end, and gracile metatarsals.

4.2 Referred Specimens

Panphagia protos, *Ch. novasi*, and *Ba. agudoensis* are known based only on their holotypes, whereas other Carnian sauropodomorphs have assigned paratypes (*Sat. tupiniquim*) or referred specimens (*E. lunensis*, *Pam. barberenai*, *Bu. schultzi*). Among these, one of the specimens referred to *Bu. schultzi* (CAPPA/UFSM 0035), one of those referred to *E. lunensis* (PVSJ 559), and one of the *Sat. tupiniquim* paratypes (MCP-PV 3845) have been extensively used to complement the holotypes when it came to scoring the respective taxon in phylogenetic analyses (Martínez et al. 2012b; Bronzati et al. 2017; Müller et al. 2018a). Instead, other referred specimens are more incomplete, including isolated femora referred to *E. lunensis* (PVSJ 852, 855 876), *Pam. barberenai* (CAPPA/UFSM 0027, 0028), and *Bu. schultzi* (ULBRA-PVT289), and an isolated axis (CAPPA/UFSM 0179) referred to the latter taxon. These assignments were mostly based on topotypy (i.e. the specimens come from the type-localities), although this does not actually apply to PVSJ 855 and 860, which came from the Valle Pintado site (see above). In fact, we agree with Sereno et al. (2012) that the referral of the isolated femora to *E. lunensis* is very tentative because this bone is unknown in *Pan. protos* and those of *Ch. novasi* are only partially preserved and crushed. This is somehow also the case for the isolated femora ascribed to *Pam. barberenai* and *Bu. schultzi*, which mostly agree in anatomy with the respective taxon, but cannot be unambiguously differentiated from all coeval taxa, from both Argentina and Brazil (but see Müller et al. 2018a). Hence, because they (1) do not significantly add to the understanding of the respective taxon with anatomical data that are not already available from more complete specimens and/or (2) are not demonstrably closer in anatomy to those taxa than to other Carnian sauropodomorphs of South America, those isolated bones are no further discussed here.

The original assignment of the syntypes of *Sat. tupiniquim* (Langer et al. 1999, 2007; Langer 2003) was also based on their general anatomical resemblances and close association (Langer 2005), as well as on their 'early sauropodomorph' phylogenetic signal. Indeed, as no coeval sauropodomorphs have been identified as such at the time, no overlap was recognised between the morphological variation within the type-series and that now recognised for the entire diversity of Carnian sauropodomorphs. This halted justifications to taxonomically split the type-material, a situation that no longer stands given the recent discovery of several coeval/similar forms. Moreover, although most skeletal parts of the type-series have been studied in detail (except for the vertebrae), a diagnosis based on apomorphies shared by the three type-specimens could not be built so far. This is in part because skeletal parts with key anatomical features (notably the skull) are not available in all specimens and also because there are indeed conspicuous differences among them.

Langer et al. (2007) noticed several similarities in the scapular girdle and forelimb of the holotype of *Sat. tupiniquim* and paratype MCP-PV 3845. In fact, they proposed an amended diagnosis based on this part of the skeleton, emphasising that the diagnostic traits are also seen in other early dinosaurs, thus not representing autapomorphies. Despite the similarities, Langer et al. (2007) listed several differences that

could be related to the more robust construction of the holotype; i.e. thicker long bone walls, broader elements such as the deltopectoral crest, the shaft and distal end of the humerus, the distal part of the femur, and the proximal portions of ulna, tibia, fibula, and metatarsals. Additional traits of the holotype pectoral skeleton, unlike that of MCP-PV 3845, include a less expanded scapular prominence, the acromion forming a lower angle to the long axis of the scapular blade, a more conspicuous coracoid tuber, a broader preglenoid ridge, and a subglenoid buttress reaching the medial margin of the coracoid (with the subglenoid fossa facing caudodorsally, and not laterally as in the paratype).

A preliminary account of the vertebral column shows that the variation in length of the presacral centra is similar in both the holotype of *Sat. tupiniquim* and paratype MCP-PV 3845. The cranial postaxial neck centra are shorter than those of the mid-cervical vertebrae, but longer than those of cranial trunk vertebrae. Yet, marked differences are seen in the sacral series; the holotype showing a caudal element incorporated into the sacrum (Langer 2003), whereas a trunk vertebra is incorporated instead in the paratype. In both specimens, the primordial sacral vertebrae are similar in shape, including their attachment to the medial surface of the ilium (Langer 2003; Marsola et al. 2018) and the incorporated vertebra, either from the trunk or tail series, bears robust transverse processes articulating with the ilium.

Other key-elements for comparison among the type-specimens of *Sat. tupiniquim* are the ilium, femur, and tibia, partially preserved in all of them. The femora are very similar, except for the absence of a trochanteric shelf in MCN-PV 3846. Otherwise, the ilia have conspicuous differences regarding the length of the postacetabular alae and the shape of the supra-acetabular crest. Indeed, the postacetabular ala of the holotype and MCN-PV 3845 are about 1.3 times longer than the space between the pre- and postacetabular embayments of the ilium (Langer and Benton 2006), a ratio that is significantly lower (slightly above. 1.0) in MCN-PV 3846. As for the supra-acetabular crest, it has a more rounded lateral profile in the holotype, whereas it is straighter and caudodorsally to cranioventrally oriented in both paratypes. Also, the fibular condyle of the tibia is more caudally placed in the paratypes, whereas the distal end of that bone is more lateromedially expanded in MCN-PV 3846 than in the holotype (this portion of the tibia is very deformed in MCN-PV 3845).

The assignment (or not) of the two more complete specimens referred to *Bu. schultzi* is more straightforward. As mentioned above, the small-sized ULBRA-PVT056 requires a more detailed analysis, but it would represent a juvenile if assigned to *Bu. schultzi*. As such, its inclusion along with ULBRA-PVT056 and CAPPA/UFSM 0035 in the phylogenetic study (see below) would patently violate the principle of not comparing different semaphoronts of the same species (Hennig 1966), hampering to elucidate the relationships of the Carnian sauropodomorphs. As for CAPPA/UFSM 0035, its assignment to *Bu. schultzi* is justified further than on topotypical principles and overall similarity with the holotype. In fact, the two specimens share a suite of traits unseen in the holotypes of other Carnian sauropododomorphs from both Brazil and Argentina (Müller et al. 2018a), including:

longer head (unlike *Ba. agudoensis*); short dorsomedial ramus of the caudal premaxillary process (unlike *E. lunensis*); lack of promaxillary fossa (unlike *Pam. barberenai*); forked part of the caudal ramus of jugal more caudally located (unlike *Pam. barberenai*); fully ziphodont maxillary and dentary 'cheek' teeth (minimally unlike *Pam. barberenai*, *Pan. protos*, and *Ba. agudoensis*); base of the scapular blade with a straight caudal margin (unlike *Sat. tupiniquim*); caudal end of the brevis shelf not projecting much more ventrally that the 'caudomedial shelf' (unlike *Pam. barberenai* and *Sat. tupiniquim*); and a rugose iliofibularis muscle insertion on the craniomedial margin of the fibula (unlike *Ch. novasi*).

A comprehensive revaluation of the more complete specimens assigned to *E. lunensis* (PVSJ 559, 745, 860, and 862; see Table 1) is a much more complex task, which is beyond the scope of the present work. PVSJ 559 was found in the same site as the holotype, and its referral to *E. lunensis* could be based on topotypy (although we endorse that such referrals should be always based on anatomy). Indeed, PVSJ 559 was assigned to *E. lunensis* by Sereno et al. (2012) also partially based on the broad proportions of its tibia and astragalus compared to those of *Pan. protos*. In fact, the astragalus and the distal end of the tibia are more transversely expanded in PVSJ 559 than in the holotype of *Pan. protos* (PVSJ 874), but this cannot be confirmed in PVSJ 512 (hootype of *E. lunensis*), because the distal end of its tibia is not fully exposed and the caudal portion of its astragalus is missing. In any case, as the distal articulation of the tibia is transversely compressed in the holotype of *Ch. novasi* (PVSJ 845), so that the opposite condition may differentiate PVSJ 559 from that taxon. Also, we agree with Sereno et al. (2012) that the ascending process and caudal fossa of the astragalus are lateromedially broader in PVSJ 559 than in PVSJ 874, and this is also the case for the incomplete astragalus of PVSJ 512. Hence, given the current diversity of the Ischigualasto Formation sauropodmormorphs, the assignment of PVSJ 559 to *E. lunensis* seems the most likely, but far from certain option.

PVSJ 745 was also referred to *E. lunensis* by Sereno et al. (2012), but with no further discussions. This specimen was not collected from the type-locality of *E. lunensis*, but from that of *Pan. protos* and *Ch. Novasi*, i.e. Valle Pintado site. It is very similar to PVSJ 512 in the shape of the basal tubera of the basioccipital, the proportions of the cervical vertebrae, femoral head and fourth trochanter anatomy (MDE pers. obs.). As for PVSJ 860 and 862, they were also collected in the Valle Pintado site. Accordingly, their referral to *E. lunensis* should be backed-up by a very detailed differentiation relative to those two other taxa. For Sereno et al. (2012), the ascending process of the astragalus of PVSJ 862 corresponds to about one-third of the width of the bone, as in PVSJ 559 and PVSJ 512, but unlike the narrower structure of PVSJ 874. In the context of the Ischigualasto Formation sauropodmormorph diversity, this could point to the affinity of PVSJ 862 to *E. lunensis*, but a more detailed evaluation of the two more complete Valle Pintado specimens assigned to that taxon is needed. This is beyond the scope of this work, so that PVSJ 860 and 862 will not be further discussed.

As briefly reviewed above, among the referred specimens of South American Carnian sauropodomorphs, the attribution of CAPPA/UFSM 0035 to *Bu. schultzi* is

relatively well supported. Yet, this is not the case of the paratypes of *Sat. tupiniquim*—which accumulate several differences relative to the holotype—neither of the specimens referred to *E. lunensis*—which lack strong anatomical evidence for their association with the holotype. Hence, their unjustified employment to complement the scoring of the respective taxon in phylogenetic datasets could lead to misleading results. Accordingly, in order to investigate the possibility that MCN-PV 3845 and 384 and PVSJ 559 and 745 do not respectively belong to *Sat. tupiniquim* and *E. lunensis*, we will run phylogenetic analyses having them as individual terminals. We will also conduct analyses with a more traditional arrangement, in which two of the more complete '*E. lunensis*' specimens (PVSJ 559, 745) and the type-series of *Sat. tupiniquim* are integrated into composite terminals. For consistency, we will also include a composite *Bu. schultzi* formed of its holotype and CAPPA/UFSM 0035, as well as with those specimens as individual terminals.

5 Phylogenetic Study

5.1 Parsimony Analyses Results

The 'specimen-based' analysis found ten most parsimonious trees (MPTs) of 1,544 steps, with a consistency index (CI) of 0.45142 and a retention index (RI) of 0.40268 (best score hit 778 times of the 1000 replicates). The strict consensus tree (Fig. 4a) shows a massive polytomy composed of *Pam. barberenai*, *Pan. protos*, *Ch. novasi*, the three specimens of *E. lunensis*, Bagualosauria, and monophyletic sets of the *Bu. schultzi* and *Sat. tupiniquim* specimens. In the alternative MPTs, *Pan. protos* may form clades with the *Eoraptor* specimens (sister to PVSJ 559), with *Sat. tupiniquim* plus Bagualosauria, or with *Pam. barberenai* plus *Ch. novasi* (as sister to the *Sat. tupiniquim* plus Bagualosauria clade). The other unstable taxon—*Ch. novasi*—is found either with *Pam. barberenai* and *Pan. protos* in a clade sister to that including all other sauropodomorphs except for the *E. lunensis* and *Bu. schultzi* sets of specimens, or in a clade with *Pam. barberenai* and the *Sat. tupiniquim* syntypes.

The a posteriori pruning of *Pan. protos* slightly improves the resolution, with the three *E. lunensis* specimens forming a clade, but with the interspecific relations among Carnian sauropodomorphs still unresolved. The additional *a posteriori* pruning of *Ch. novasi* results in a trichotomy composed of monophyletic sets of *E. lunensis* and *Bu. schultzi* specimens, plus a clade of more deeply nested sauropodomorphs (Fig. 4b). The latter includes a trichotomy formed by *Pam. barberenai*, the *Sat. tupiniquim* clade, and Bagualosauria. Bremer supports for the *E. lunensis* and *Bu. schultzi* clades are minimal, as it is also the case for the clade that includes *Pam. barberenai*, the *Sat. tupiniquim* clade, and Bagualosauria. Similarly, the bootstrap frequencies of these branches are below 50%, with exception of those of the *Bu. schultzi* clade. Bremer supports and absolute bootstrap frequencies

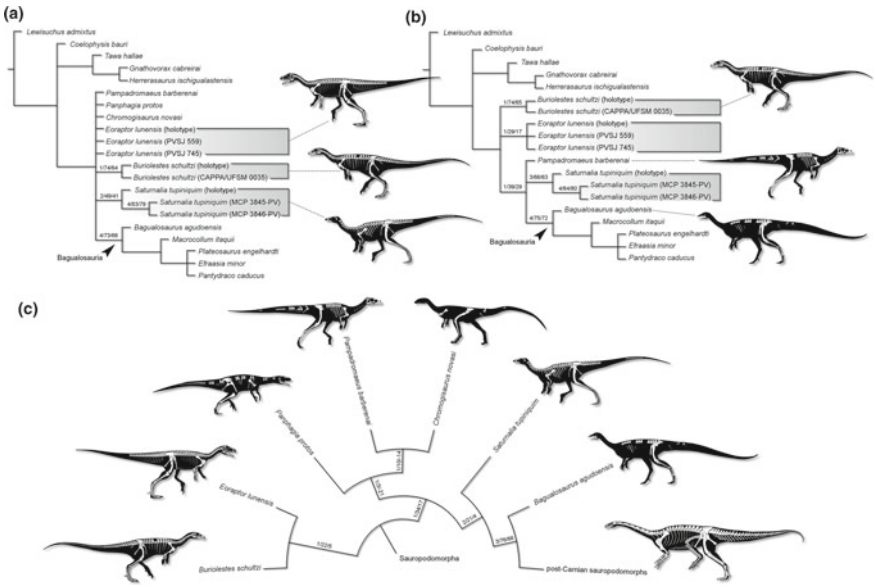

Fig. 4 Phylogenetic relations of the Carnian sauropodomorphs. **a** Strict consensus tree of the 'specimen-based' analysis. **b** Strict reduced consensus tree of the 'specimen-based' analysis with the a posteriori pruning of *Panphagia protos* and *Chromogisaurus novasi*. **c** single MPT of the 'combined' analysis

of Bagualosauria and the *Sat. tupiniquim* clade are higher: 3/66% and 4/75%, respectively. Finally, it is interesting to note that the branch support of the clade composed of the two paratypes of *Sat. tupiniquim*—MCP 3845-PV and MCP 3846-PV—is very high, with a Bremer support of 4 and an absolute bootstrap frequency of 84%.

The 'combined' analysis found a single MPT of 1,453 steps with a consistency index (CI) of 0.47970 and a retention index (RI) of 0.38286 (best score hit 713 times of the 1000 replicates). In the fully resolved optimal tree (Fig. 4c), *Bu. schultzi* and *E. lunensis* are joined in a clade sister to all other Sauropodomorpha. *Pan. protos* is found as a sister to *Pam. barberenai* plus *Ch. novasi*, in a clade sister to that including *Sat. tupiniquim* plus Bagualosauria. Bremer supports are usually minimal along the part of the tree that includes Carnian sauropodomorphs, with the exception of Bagualosauria and the clade it forms with *Sat. tupiniquim*, which have decay indices of 3 and 2, respectively. Similarly, bootstrap frequencies are all lower than 50%, except for those of Bagualosauria, which has absolute and GC frequencies of 76% and 66%, respectively.

We found the following results under constrained topologies: one additional step is necessary to force the position of *Bu. schultzi* as the earliest-diverging sauropodomorph; two extra steps are required to force the sister taxon relationships between *Sat. tupiniquim* and *Ch. novasi*, between *Sat. tupiniquim* and *Pam. barberenai*, and between *E. lunensis* and *Pan. protos*, as well as to form a clade composed of the three Ischigualastian species; nine extra steps are needed to recover

Pam. barberenai as the sister taxon to *Ba. agudoensis*. Finally, only Bagualosauria and its clade with *Sat. tupiniquim* are found in the strict consensus tree generated from suboptimal trees one step longer than the MPTs, with all other interrelations among Carnian sauropodomorphs being unresolved.

5.2 Carnian Sauropodomorph Relationships

The above results reveal that there is no disagreement between phylogenetic hypotheses when the three taxa with multiple specimens—*Sat. tupiniquim*, *E. lunensis*, and *Bu. Schultzi*—are analysed based on either their assigned specimens or combined scorings. Indeed, although the strict consensus tree of Fig. 4a is much less resolved than that of Fig. 4c, they show no conflict and at least concur in those three taxa (as well as *Pam. barberenai*, *Pan. protos*, and *Ch. novasi*) are external to Bagualosauria. Moreover, the specimens of *Bu. schultzi* and *Sat. tupiniquim* form clades, so that their assignment to the respective taxon is backed up by this phylogenetic study (see below for *E. lunensis*). Hence, our more conservative result—i.e. the strict consensus tree of the 'specimen-based' analysis—answers three of our proposed questions, supporting the monophylies of *Sat. tupiniquim* and *Bu. schultzi* (as composed of their specimens included in this analysis), as well as that of Bagualosauria (as composed of post-Carnian sauropodomorphs plus *Ba. agudoensis*, but no other Carnian taxon). The latter hypothesis agrees with most phylogenetic arrangements proposed so far (but see Müller and Garcia 2020) and may be considered a settled issue based on the currently available evidence.

The sister-group relation between *Ba. agudoensis* and post-Carnian sauropodomorphs, forming Bagualosauria, is supported in the present study by a series of synapomorphies, the most noteworthy of which are (see complete list in the Supplementary Material): larger size; inset first dentary tooth (also seen in *Pan. protos* and *E. lunensis*); ventrally curved rostral end of dentary; 'cheek tooth' crowns with enlarged denticles (also seen in *Pam. barberenai* and *E. lunensis*); smooth medial surface of the proximal portion of fibula (also seen in *E. lunensis*). As for the grouping of the two *Bu. schultzi* specimens into a clade, this is supported by a single trait in the analysis: concave area above supra-acetabular crest restricted to the dorsal half of the iliac blade. Yet, the status of that feature as autapomorphic for the species is jeopardised by its presence also in other Carnian sauropodomorphs.

Regarding *Sat. tupiniquim*, the apomorphies that group its syntypes are: dorsoventrally shallow sacral ribs; ventral surface of proximal caudal centra keeled or strongly constricted lateromedially; crested craniolateral margin of femoral shaft proximal portion. The latter two traits are also seen in other Carnian sauropodomorphs, so that our study also did not reveal a convincing set of autapomorphies for *Sat. tupiniquim.* Interestingly, the grouping of the two *Sat. tupiniquim* paratypes into a minimal clade is supported by a broader array of features, including a caudoventrally oriented ischiadic peduncle of the ilium, a more craniocaudaly elongated lateral condyle of the femur, a fibular shaft with a more marked insertion of m. iliofibularis, a cranially

straight cnemial crest of the tibia, and a distal end of the tibia that is lateromedially broader, has an acute craniomedial corner, and lacks a proximodistaly elongated ridge on the medial portion of its caudal surface.

Pruned of the more volatile *Pan. protos* and *Ch. novasi*, the topology of Fig. 4b agrees with that of the 'combined' analysis (Fig. 4c) in that *E. lunensis* and *Bu. schultzi* are external to a clade that includes *Sat. tupiniquim*, *Pam. barberenai*, and bagualosaurs. In addition, the specimens assigned to *E. lunensis* now form a clade. This answers two further questions, supporting the monophyly of *E. lunensis* (as composed of the three specimens analysed here) and a more 'pectinate' phylogenetic arrangement for early sauropodomorphs. Indeed, some studies suggested that all Carnian sauropodomorphs (except for *Ba. agudoensis*) form a clade exclusive of other members of the group (Martínez et al. 2011; Langer et al. 2017; Baron et al. 2017a; Müller et al. 2018a). Even if this is still a possibility based on the topology of Fig. 4a, those of Fig. 4b, c indicate otherwise. As such, we understand that the present study provides reasonable evidence against a clade grouping all non-bagualosaur sauropodomorphs, suggesting instead the 'higher-nesting' of some taxa in the direction of Bagualosauria.

The nesting of *Sat. tupiniquim* and *Pam. barberenai* in a clade with bagualosaurs to the exclusion of *E. lunensis* and *Bu. schultzi* is supported in the present studies by a series of synapomorphies (see Supplementary Material), including portion of the lacrimal lateral lamina covering the antorbital fossa positioned at the mid-length of its caudal margin, tooth crowns labio lingually and mesiodistally expanded at base, and 'cheek tooth' crowns with a convex basal half of the distal margin. Besides, the grouping of the three specimens of *E. lunensis* analysed here is supported by epipophyses limited to more cranial postaxial cervical vertebrae, trunk vertebrae lacking prezygoparapophyseal laminae, and ilium with the lateral tip of the supra-acetabular crest closer to ischiadic peduncle and smooth origins for mm. flexor tibialis and iliotibialis. Interestingly, the latter three features are shared only by *Pan. protos* among Carnian sauropodomorphs, matching the possible affinity of those two Ischigualasto taxa as seen in some MPTs of the 'specimen-based' analysis.

The best resolution of the phylogenetic hypotheses presented here is that resulting from the 'combined' analysis. Apart from agreeing with the arrangements seen in the 'specimen-based' results (Fig. 4a, b), that topology reveals further hypotheses of relationships (Fig. 4c), including the sister-group relations between *E. lunensis* and *Bu. schultzi*. This has never been previously proposed, but is supported in our study by several synapomorphies, the most noteworthy of which are (see complete list in the Supplementary Material): a longer dorsolateral process of the premaxillary caudal ramus; a maxilla not significantly contributing to the external naris; a rugose ridge on the laterodorsal corner of the lacrimal rostral ramus; lacrimal with ventral ramus broader that the rostral; lacrimal with a lateral lamina covering part of the internal antorbital fenestra; ventral ramus of postorbital with a rostrally deflected end; a caudal vertebra incorporated into the sacrum; cranial margin of scapular blade not markedly concave; a stouter pubic peduncle of the ilium.

The topology of Fig. 4b already placed *Sat. tupiniquim* and *Pam. barberenai* in a clade with bagualosaurs, exclusive of *E. lunensis* and *Bu. schultzi*. Yet, the

'combined' analysis also includes *Pan. protos* and *Ch. novasi* into that clade, which is supported by the following main synapomorphies (see full list in the Supplementary Material): no diastema between last premaxillary and first maxillary alveoli, large and rostrally opened foramen perforating the lateral surface of the base of the maxillary ascending process, portion of the lacrimal lateral lamina covering the antorbital fossa positioned at the mid-length of its caudal margin, more laterally positioned paraquadratic foramen, deeper postdentary portion of lower jaw, tooth crowns labio lingually and mesiodistally expanded at base, higher tooth crowns in the rostral quarter of the tooth series, first premaxillary tooth crown with smooth carena, 'cheek tooth' crowns with a reduced distal concavity of the long axis and a convex basal half of the distal margin, pointed or right angled apex of deltopectoral crest, pubic shaft with nearly straight outline in lateral/medial views, distal end of tibia with more oblique facet for reception of ascending process of astragalus, and pedal digit II with ungual phalanx longer than second phalanx. Indeed, the placement of *E. lunensis* and *Bu. schultzi* outside a clade including all other sauropodomorphs is replicated in several previous phylogenetic analyses and is the arrangement favoured by the present investigation.

The 'combined' analysis (Fig. 4c) also identified a sister-group relation between *Sat. tupiniquim* and Bagualosauria. In most previous studies in which *Sat. tupiniquim* appears closely related to bagualosaurs, it forms a minimal clade with *Ch. novasi*. In fact, very few phylogenetic analyses (e.g. Bittencourt et al. 2015) found *Sat. tupiniquim* closer to Norian sauropodomorphs than to *Ch. novasi*. Here, this relation was supported by the following main synapomorphies (see the Supplementary Material for a complete list): smaller head; prefrontal lacking a bone sheet expanding rostroventrally from the intersection of rostral and ventral processes; broader interorbital portion of the frontal; stouter dentary; diapophysis and parapophysis nearly touching in cervical vertebrae 3–7; proximal surface of metatarsal II with a non-concave lateral margin; metatarsal III narrower caudally than cranially in proximal outline. Yet, it is important to mention that *Ch. novasi* does not preserve the skeletal parts related to any of those features, so that its closer relation to *Sat. tupiniquim* cannot be fully discarded based only on the results of this phylogenetic study.

Sister to *Sat. tupiniquim* plus Bagualosauria, the combined analysis recovered a clade composed of the 'lesser-known' Carnian sauropodomorphs, i.e. *Pan. protos*, *Ch. novasi*, and *Pam. barberenai*. This is supported by a paraquadratic foramen almost fully enclosed within the quadrate, an everted caudolateral margin of the quadrate creating a caudally facing fossa, and a relatively stouter tibia, the distal end of which has a concave caudal margin. In addition, some synapomorphies place *Pam. barberenai* and *Ch. novasi* more closely related to one another, including a relatively deeper ilium and acetabulum, a sharp dorsal margin of the iliac pubic peduncle, and a straight ventral margin of iliac acetabular wall. A close relation between *Pan. protos* and *Pam. barberenai* was already proposed by some authors (Müller et al. 2018a; Bronzati et al. 2019a; Pacheco et al. 2019; Müller and Garcia 2020), but never along with *Ch. novasi*. In fact, the overall weak support of the 'combined' analysis results shows that these relations have to be considered with care. Indeed, alternative arrangements revealed by some MPTs of the 'specimen-based' analysis include the position of *Pan. protos*

both within the set of *E. lunensis* specimens or more highly nested, close to the Bagualosauria plus *Sat. tupiniquim* clade. The first of those hypotheses would indicate that either these two taxa are synonymous or that some *E. lunensis* specimens may actually belong to *Pan. protos*. As for *Ch. novasi*, it may form a clade with *Pam. barberenai* and *Sat. tupiniquim,* but was not found closer to the latter taxon in any of the MPTs, as it has been frequently suggested in previous studies.

6 Morphological Disparity Analysis

The morphospace generated from the first and second PCos (22.39% and 19.16% of variance, respectively) separated the hypodigms of *E. luensis*, *Sat. tupiniquim*, and *Bu. schultzi* into distinct clusters (Fig. 5a). *Eoraptor lunensis* specimens are positioned on the upper left quadrant, *Bu. schultzi* specimens on the lower left quadrant, and those of *Sat. tupiniquim* on the lower right quadrant of the morphospace. *Chromogisaurus novasi* is found closer to the *Bu. schultzi* cluster than to other taxa in the first two PCos, whereas *Pan. protos* and *Pam. barberenai* are positioned very close to one another and well separated from all other species in the same axes. *Bagualosaurus agudoensis* is the closest species to the latter two, within the upper right corner of the morphospace.

The generalised least squares regression between the values of the first three PCos and the logarithm of femoral length (as a proxy of body size) did not recover a significant regression for any of the PCos ($p > 0.14$), indicating that body size does not explain the morphospacial structure (Fig. 5b). The PERMANOVA found a

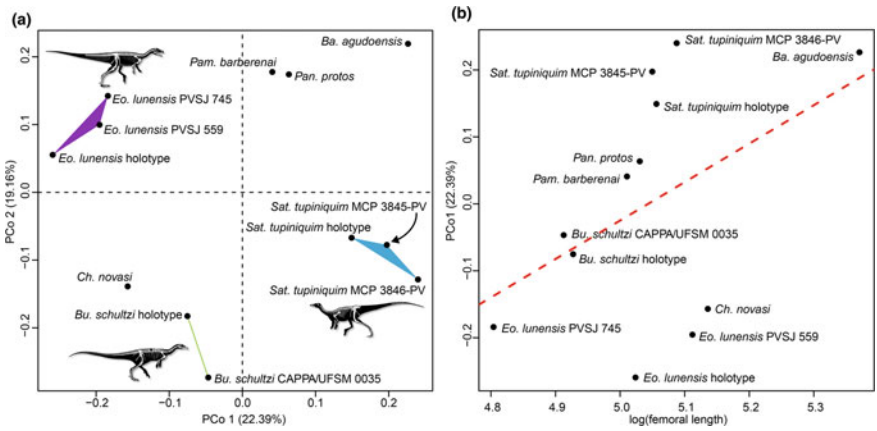

Fig. 5 Morphospace of the Carnian sauropodomorphs. **a** Morphospace represented by PCo1 and PCo2, hypodigms composed of more than one specimen highlighted by coloured convex hulls. **b** log(femoral length), as proxy of body size, versus PCo1 showing the non-significant linear regression (red dotted line) between both variables

significant difference ($p = 0.04107$) between the three hypodigms of *E. luensis*, *Sat. tupiniquim*, and *Bu. schultzi*. Similarly, the LDA predicted correctly the assignment of each specimen to its respective species with posterior probabilities ≥ 0.99.

The morphospace and statistical analyses derived from it provide strong support for the assignment of the evaluated specimens of *E. luensis*, *Sat. tupiniquim*, and *Bu. schultzi* to the respective species. This agrees with the results of the 'specimen-based' phylogeny for the two latter taxa (Fig. 4a) and helps support the assignment of PVSJ 559 and 745 to *E. lunensis*, which was only phylogenetically supported when *Pan. protos* was excluded from the analysis (Fig. 4b). The morphological disparity analysis takes into account overall dissimilarity and not only apomorphic conditions, contrasting with the phylogenetic analysis. Thus, they are complementary, distinguishing species based on unique combinations of character states (disparity analysis) and autapomorphies (phylogenetic analysis). In the end, this distance matrix-based analysis could be also potentially useful to explore the alpha-taxonomy of Carnian sauropodomorphs when new specimens are available.

7 Conclusions

- The holotypes of the seven Carnian sauropodomorphs of South America—*Ba. agudoensis*, *Bu. schultzi*, *Ch. novasi*, *E. lunensis*, *Pam. barberenai*, *Pan. protos*, and *Sa. tupiniquim*—can be anatomically differentiated from one another, hence supporting the taxonomic validity of the species they represent.
- A specimen-based phylogenetic analysis supports the referral of the *Sa. tupiniquim* paratypes and the best-preserved specimen referred to *Bu. schultzi* to the respective species. This is also supported by topotypy, anatomical congruence (especially for *Bu. schultzi*), and their statistically significant groupings in the distance matrix-based morphospace generated from the same dataset as the phylogenetic analysis.
- The referral of the various specimens previously assigned to *E. lunensis* is not supported by strong anatomical congruence and neither (for some specimens) on topotypy. Some of these specimens share putative autapomorphies with the holotype, as well as unique features relative to other Ischigualasto dinosaurs. Two of them nested close to the holotype in our morphospace analysis, but the specimen-based phylogenetic analysis failed to strongly support their affinity. In some resulting MPTs, *Pan. protos* was positioned within the clade of *E. lunensis* specimens, calling for a much-needed taxonomic revision of the specimens referred to that taxon.
- All phylogenetic analyses conducted here support the sister-group relation between *Ba. agudoensis* and post-Carnian sauropodomorphs (forming Bagualosauria). They less strongly support the hypotheses that *Bu. schultzi* and *E. lunensis* represent the earliest branches of Sauropodomorpha and that *Sa. tupiniquim* and *Pam. barberenai* are more highly nested in the direction of Bagualosauria.

- A species-level phylogenetic analysis further indicates that *Bu. schultzi* and *E. lunensis* form a clade, that *Sa. tupiniquim* is the sister taxon to Bagualosauria, and that *Pan. protos*, *Ch. novasi*, and *Pam. barberenai*, also form a clade. These clades are, however, not strongly supported by robustness measurements in the phylogenetic tree, warranting that more research is needed to untangle their relations.
- Alternative relations emerging from subsets of MPTs include the proximity of *Pan. protos* to either *E. lunensis* or Bagualosauria and a possible clade formed by *Sat. tupiniquim*, *Ch. novasi*, and *Pam. barberenai*, also requiring further investigation.

Acknowledgements This study was partially funded by São Paulo Research Foundation (FAPESP 2020/07997-4 to MCL and 2018/18145-9 to M.B.), Agencia Nacional de Promoción Científica y Técnica (PICT 2018-01186 to MDE), Coordenação de Aperfeiçoamento de Pessoal de Nível Superior (CAPES 88887.572782/2020-00 to J.C.A.M.), Fundação de Amparo à Pesquisa do Estado do Rio Grande do Sul (FAPERGS 21/2551-0000680-3 to R.T.M.), and Concelho Nacional de Desenvolvimento Científico e Tecnológico and Fundação de Amparo à Pesquisa do Estado de Minas Gerais (FAPEMIG PPM-00304-18 to J.S.B.). Access to the free version of TNT 1.5 was possible due to the Willi Henning Society.

Supplementary Information Available at: https://osf.io/h8qs3/?view_only=3100c6a2c8d54e9aa91fbf6655f9a2df

References

Agnolín FL, Rozadilla S (2018) Phylogenetic reassessment of *Pisanosaurus mertii* Casamiquela 1967 a basal dinosauriform from the Late Triassic of Argentina. J Sys Palaeontol 16(10):853–879

Alcober OA, Martínez RN (2010) A new herrerasaurid (Dinosauria Saurischia) from the Upper Triassic Ischigualasto formation of northwestern Argentina. ZooKeys 63:55–81

Apaldetti C, Martínez RN, Alcober OA, Pol D (2011) A new basal sauropodomorph (Dinosauria: Saurischia) from Quebrada del Barro Formation (Marayes–El Carrizal Basin) northwestern Argentina. PLoS One 6(11):e26964

Baron MG (2019) *Pisanosaurus mertii* and the Triassic ornithischian crisis: could phylogeny offer a solution? Hist Biol 31(8):967–981

Baron MG, Barrett PM (2017) A dinosaur missing–link? *Chilesaurus* and the early evolution of ornithischian dinosaurs. Biol Lett 13(8):20170220

Baron MG, Williams ME (2018) A re–evaluation of the enigmatic dinosauriform *Caseosaurus crosbyensis* from the Late Triassic of Texas USA and its implications for early dinosaur evolution. Acta Palaeontol Pol 63:129–145

Baron MG, Norman DB, Barrett PM (2017a) Baron et al reply Nature 551(7678):E4–E5

Baron MG, Norman DB, Barrett PM (2017b) A new hypothesis of dinosaur relationships and early dinosaur evolution. Nature 543(7646):501–506

Barrett PM, Upchurch P (2007) The evolution of feeding mechanisms in early sauropodomorph dinosaurs. Spec Pap Palaeontol 77:91–112

Barrett PM, Upchurch P, Zhou XD, Wang XL (2007) The skull of *Yunnanosaurus huangi* Young 1942 (Dinosauria: Prosauropoda) from the Lower Lufeng Formation (Lower Jurassic) of Yunnan China. Zool J Linn Soc 150(2):319–341

Benson RBJ, Campione NE, Carrano MT, Mannion PD, Sullivan C, Upchurch P, Evans DC (2014) Rates of Dinosaur Body Mass Evolution Indicate 170 Million Years of Sustained Ecological Innovation on the Avian Stem Lineage. PLoS Biol 12(5):e1001853

Bittencourt JS, Arcucci AB, Marsicano CA, Langer MC (2015) Osteology of the Middle Triassic archosaur *Lewisuchus admixtus* Romer (Chañares Formation Argentina) its inclusivity and relationships amongst early dinosauromorphs. J Sys Palaeontol 13(3):189–219

Bonaparte JF, Ferigolo J, Ribeiro AM (1999) A new early Late Triassic saurischian dinosaur from Rio Grande do Sul state, Brazil. Nat Sci Mus Monogr 15:89–109

Bremer K (1988) The limits of amino acid sequence data in angiosperm phylogenetic reconstruction. Evolution 42:795–803

Bremer K (1994) Branch support and tree stability. Cladistics 10:295–304

Bronzati M, Rauhut OW, Bittencourt JS, Langer MC (2017) Endocast of the Late Triassic (Carnian) dinosaur *Saturnalia tupiniquim*: implications for the evolution of brain tissue in Sauropodomorpha. Sci Rep 7(1):1–7

Bronzati M, Rauhut OW (2018) Braincase redescription of *Efraasia minor* Huene 1908 (Dinosauria: Sauropodomorpha) from the Late Triassic of Germany with comments on the evolution of the sauropodomorph braincase. Zool J Linn Soc 182(1):173–224

Bronzati M, Benson RB, Rauhut OW (2018) Rapid transformation in the braincase of sauropod dinosaurs: integrated evolution of the braincase and neck in early sauropods? Palaeontology 61(2):289–302

Bronzati M, Müller RT, Langer MC (2019a) Skull remains of the dinosaur *Saturnalia tupiniquim* (Late Triassic, Brazil): With comments on the early evolution of sauropodomorph feeding behaviour. PLoS OONE 221:e0221387.

Bronzati M, Langer MC, Rauhut OWM (2019b) Braincase anatomy of the early sauropodomorph *Saturnalia tupiniquim* (Late Triassic, Brazil). J Vert Paleontol 38(5): https://doi.org/10.1080/02724634.2018.1559173

Cabreira SF, Schultz CL, Bittencourt JS, Soares MB, Fortier DC, Silva LR, Langer MC (2011) New stem-sauropodomorph (Dinosauria Saurischia) from the Triassic of Brazil. Naturwissenschaften 98(12):1035–1040

Cabreira SF, Kellner AWA, Dias-da-Silva S, da Silva LR, Bronzati M, Marsola JC, Müller RT, Bittencourt JS, Batista B, Raugust T, Carrilho R, Brodt A, Langer MC (2016) A unique Late Triassic dinosauromorph assemblage reveals dinosaur ancestral anatomy and diet. Curr Biol 26(22):3090–3095

Campione NE, Evans DC, Brown CM, Carrano MT (2014) Body mass estimation in non-avian bipeds using a theoretical conversion to quadruped stylopodial proportions. Methods Ecol Evol 5:913–923

Cau A (2018) The assembly of the avian body plan: a 160–million–year long process. Boll Soc Paleontol Ital 57(1):1–25

Cerda IA, Chinsamy A, Pol D, Apaldetti C, Otero A, Powell JE, Martínez RN (2017) Novel insight into the origin of the growth dynamics of sauropod dinosaurs. PLoS ONE 12(6): e0179707

Chapelle KE, Choiniere JN (2018) A revised cranial description of *Massospondylus carinatus* Owen (Dinosauria: Sauropodomorpha) based on computed tomographic scans and a review of cranial characters for basal Sauropodomorpha. PeerJ 6:e4224

Chapelle KE, Barrett PM, Botha J, Choiniere JN (2019) Ngwevu intloko: a new early sauropodomorph dinosaur from the Lower Jurassic Elliot Formation of South Africa and comments on cranial ontogeny in *Massospondylus carinatus*. PeerJ 7:e7240

Chatterjee S (1987) A new theropod dinosaur from India with remarks on the Gondwana-Laurasia connection in the Late Cretaceous. In McKenzie GD (ed.). Gondwana 6: Stratigraphy, Sedimentology, and Paleontology. Geophy Monogr 41:183–189

Coddington JA, Scharff N (1994) Problems with zero-length branches. Cladistics 10:415–423

Colombi C, Martínez RN, Césari SN, Alcober O, Limarino CO, Montañez I. (2021). A high-precision U–Pb zircon age constraints the timing of the faunistic and palynofloristic events of the Carnian Ischigualasto Formation, San Juan, Argentina. J South Am Earth Sci 111: 103433

Da Rosa AAS (2015) Geological context of the dinosauriform-bearing outcrops from the Triassic of Southern Brazil. J South Am Earth Sci 61:108–119

Dal Sasso C, Maganuco S, Cau A (2018) The oldest ceratosaurian (Dinosauria: Theropoda) from the Lower Jurassic of Italy sheds light on the evolution of the three–fingered hand of birds. PeerJ 6:e5976

Delcourt R, Azevedo SAK, Grillo ON, Deantoni FO (2012) Biomechanical comments about Triassic dinosaurs from Brazil. Pap Avulsos Zool 52:341–347

Desojo JB, Fiorelli LE, Ezcurra MD, Martinelli AG, Ramezani J, Da Rosa AAS, Baczko MB, Trotteyn MJ, Montefeltro FC, Ezpeleta M, Langer MC (2020) The Late Triassic Ischigualasto Formation at Cerro Las Lajas (La Rioja, Argentina): fossil tetrapods, high-resolution chronostratigraphy, and faunal correlations. Sci Rep 10:12782

Ezcurra MD (2006) A review of the systematic position of the dinosauriform archosaur *Eucoelophysis baldwini* Sullivan Lucas 1999 from the Upper Triassic of New Mexico USA. Geodiversitas 28(4):649–684

Ezcurra MD (2010) A new early dinosaur (Saurischia: Sauropodomorpha) from the Late Triassic of Argentina: a reassessment of dinosaur origin and phylogeny. J Sys Palaeontol 8(3):371–425

Ezcurra MD (2012a) Comments on the taxonomic diversity and paleobiogeography of the earliest known dinosaur assemblages (late Carnian-earliest Norian). Hist Nat 2:49–71

Ezcurra MD (2012b) Sistemática, biogeografía y patrones macroevolutivos de los dinosaurios terópodos del Triásico Tardío y Jurásico Temprano. Universidad de Buenos Aires, Buenos Aires, Tesis de Licenciatura, p 512

Ezcurra MD, Novas FE (2007) Phylogenetic relationships of the Triassic theropod *Zupaysaurus rougieri* from NW Argentina. Hist Biol 19(1):35–72

Ezcurra MD, Fiorelli LE, Martinelli AG, Rocher S, von Baczko MB, Ezpeleta M, Taborda JRA, Hechenleitner EM, Trotteyn MJ, Desojo JB (2017) Deep faunistic turnovers preceded the rise of dinosaurs in southwestern Pangaea. Nat Ecol Evol 1:1477–1483

Ezcurra MD, Nesbitt SJ, Bronzati M, Dalla Vecchia FM, Agnolin FL, Benson RBJ, Egli FB, Cabreira SF, Evers SW, Gentil AR, Irmis RB, Martinelli AG, Novas FE, Roberto da Silva L, Smith ND, Stocker MR, Turner AH, Langer MC (2020a) Enigmatic dinosaur precursors bridge the gap to the origin of Pterosauria. Nature 588:445–449

Ezcurra MD, Nesbitt SJ, Fiorelli LE, Desojo JB (2020b) New specimen sheds light on the anatomy and taxonomy of the early Late Triassic dinosauriforms from the Chañares Formation, NW Argentina. Anat Rec 303:1393–1438

Fabbri M, Tschopp E, McPhee B, Nesbitt S, Pol D, Langer MC (2020) Sauropodomorpha F. R. von Huene. In de Queiroz K, Cantino PD, Gauthier JA (eds,) Phylonyms: a Companion to the PhyloCode p:1225–1234. CRC Press

Felsenstein J (1985) Confidence limits on phylogenies: an approach using the bootstrap. Evolution 39:783–791

Ferreira-Cardoso S, Araújo R, Martins NE, Martins GG, Walsh S, Martins RMS, Kardjilov N, Manke I, Hilger A, Castanhinha R (2017) Floccular fossa size is not a reliable proxy of ecology and behaviour in vertebrates. Sci Rep 7(2005):s41598–017–01981–0

Fraser NC, Padian K, Walkden GM, Davis ALM (2002) Basal dinosauriform remains from Britain and the diagnosis of the Dinosauria. Palaeontology 45(1):79–95

Galton PM, Upchurch P (2004) Prosauropoda. In Weishampel DB, Dodson P, Osmolska H (eds) The Dinosauria (Second Edition) University of California Press Berkeley p232–258

Garcia MS, Müller RT, Pretto FA, Da-Rosa AAS, Dias-Da-Silva s (2021) Taxonomic and phylogenetic reassessment of a large-bodied dinosaur from the earliest dinosaur-bearing beds (Carnian, Upper Triassic) from southern Brazil. J Syst Palaeontol DOI: https://doi.org/10.1080/14772019.2021.1873433

Garcia MS, Pretto FA, Dias-Da-Silva S, Müller RT (2019) A dinosaur ilium from the Late Triassic of Brazil with comments on key–character supporting Saturnaliinae. An Acad Bras Ciênc 91:1–20

Gauthier JA, Langer MC, Novas FE, Bittencourt JS, Ezcurra MD (2020) Saurischia H. G. Seeley. In de Queiroz K, Cantino PD, Gauthier JA (eds,) Phylonyms: a Companion to the PhyloCode p:1219–1224. CRC Press

Godoy MM, Scherer OLB, Binotto RB, Kisvhlat EE, Dreher AM (2018) Geologia e Recursos Minerais da folha Santa Maria SH.22-V-C-IV: estado do Rio Grande do Sul. CPRM, Porto Alegre

Goloboff P, Catalano SA (2016) TNT version 1.5, including a full implementation of phylogenetic morphometrics. Cladistics 32(3):221–238

Goloboff PA, Farris JS, Nixon KC (2008) TNT a free program for phylogenetic analysis. Cladistics 24(5):774–786. https://doi.org/10.1111/j.1096-0031.2008.00217.x

Goloboff P, Farris J, Nixon K (2003a) T.N.T.: Tree Analysis Using New Technology. Program and documentation, available at http://www.zmuc.dk/public/phylogeny/tnt

Goloboff PA, Farris JS, Källersjö M, Oxelman B, Ramírez M, Szumik C (2003b) Improvements to resampling measures of group support. Cladistics 19:324–332

Griffin CT, Munyikwa D, Broderick TJ, Tolan S, Zondo M, Nesbitt SJ, Taruvinga H (2018) An exceptional new Late Triassic (Carnian) fossil assemblage from Zimbabwe and the biogeography of the earliest dinosaurs across Pangea. Society of Vertebrate Paleontology Meeting Program and Abstracts (Albuquerque, NM) p.137

Hennig EHW (1966) Phylogenetic Systematics. University of Illinois Press, Urbana

Horn BLD, Melo TM, Schultz CL, Philipp RP, Kloss HP, Goldberg K (2018) A new third-order sequence stratigraphic framework applied to the Triassic of the Parana Basin, Rio Grande do Sul, Brazil, based on structural, stratigraphic and paleontological data. J South Am Earth Sci 55:123–132

Irmis RB, Nesbitt SJ, Padian K, Smith ND, Turner AH, Woody D, Downs A (2007) A Late Triassic dinosauromorph assemblage from New Mexico and the rise of dinosaurs. Science 317(5836):358–361

Langer MC (2003) The pelvic and hindlimb anatomy of the stem-sauropodomorph *Saturnalia tupiniquim* (Late Triassic, Brazil). PaleoBios 23:1–40

Langer MC (2004) Basal Saurischia. In Weishampel DB, Dodson P, Osmolska H (eds) The Dinosauria (Second Edition) University of California Press Berkeley p25–46

Langer MC (2005) Studies on continental Late Triassic tetrapod biochronology. I. The type locality of *Saturnalia tupiniquim* and the faunal succession in south Brazil. J South Am Earth Sci 19:205–218

Langer MC, Benton MJ (2006) Early dinosaurs: a phylogenetic study. J Sys Palaeontol 4(4):309–358

Langer MC, Abdala F, Richter M, Benton MJ (1999) A sauropodomorph dinosaur from the Upper Triassic (Carman) of southern Brazil. CR Acad Sci IIA 329(7):511–517

Langer MC, França MAG, Gabriel S (2007) The pectoral girdle and forelimb anatomy of the stem-sauropodomorph *Saturnalia tuiniquim* (Upper Triassic, Brazil). Spec Pap Palaeontol 77:113–137

Langer MC, Ezcurra M, Bittencourt JS, Novas F (2009) The origin and early evolution of dinosaurs. Biol Rev 85:55–110

Langer MC, Bittencourt JS, Schultz CL (2011) A reassessment of the basal dinosaur *Guaibasaurus candelariensis* from the Late Triassic Caturrita Formation of south Brazil. Earth Environ Sci Trans R Soc Edinb 101(3–4):301–332

Langer MC, Ezcurra M, Rauhut OW, Benton MJ, Knoll F, McPhee BW, Brusatte SL (2017) Untangling the dinosaur family tree. Nature 551(7678):E1–E3

Langer MC, Ramezani J, Da Rosa AAS (2018) U-Pb age constraints on dinosaur rise from south Brazil. Gondwana Res 57:133–140

Langer MC, McPhee BW, Marsola JC, Roberto-da-Silva L, Cabreira SF (2019) Anatomy of the dinosaur *Pampadromaeus barberenai* (Saurischia—Sauropodomorpha) from the Late Triassic Santa Maria Formation of southern Brazil. PloS one 14(2):e0212543

Langer MC, Novas FE, Bittencourt JS, Ezcurra MD, Gauthier JA (2020) Dinosauria R. Owen. In de Queiroz K, Cantino PD, Gauthier JA (eds,) Phylonyms: a Companion to the PhyloCode p:1209–1217. CRC Press

Lehmann OE, Ezcurra MD, Butler RJ, Lloyd GT (2019) Biases with the generalized euclidean distance measure in disparity analyses with high levels of missing data. Palaeontol 62(5) 837–849. https://doi.org/10.1111/pala.12430

Lloyd GT (2016) Estimating morphological diversity and tempo with discrete character-taxon matrices: implementation, challenges, progress, and future directions. Biol J Linn Soc 118:131–151

Marsh AD, Rowe TB (2018) Anatomy and systematics of the sauropodomorph *Sarahsaurus aurifontanalis* from the Early Jurassic Kayenta Formation. PloS one 13(10):e0204007

Marsh AD, Parker WG, Langer MC, Nesbitt SJ (2019) Redescription of the holotype specimen of *Chindesaurus bryansmalli* Long and Murry 1995 (Dinosauria Theropoda) from Petrified Forest National Park Arizona. J Vert Paleontol 39(3):e1645682

Marsola JC, Bittencourt JS, Butler RJ, Da-Rosa ÁA, Sayão JM, Langer MC (2018) A new dinosaur with theropod affinities from the Late Triassic Santa Maria Formation South Brazil. J Vert Paleontol 38(5):e1531878

Martínez RN (2009) *Adeopapposaurus mognai* gen et sp nov (Dinosauria: Sauropodomorpha) with comments on adaptations of basal Sauropodomorpha. J Vert Paleontol 29(1):142–164

Martínez RN, Alcober OA (2009) A basal sauropodomorph (Dinosauria: Saurischia) from the Ischigualasto Formation (Triassic Carnian) and the early evolution of Sauropodomorpha. PLoS One 4(2):e4397

Martínez RN, Sereno PC, Alcober OA, Colombi CE, Renne PR, Montañez IP, Currie BS (2011) A basal dinosaur from the dawn of the dinosaur era in southwestern Pangaea. Science 331(6014):206–210

Martínez RN, Apaldetti C, Alcober OA, Colombi CE, Sereno PC, Fernandez E, Malnis PS, Correa GA, Abelin D (2012a) Vertebrate succession in the Ischigualasto Formation. J Vert Paleontol 32(sup1):10–30

Martínez RN, Apaldetti C, Abelin D (2012b) Basal sauropodomorphs from the Ischigualasto Formation. J Vert Paleontol 32(sup1):51–69

Martínez RN, Haro JA, Apaldetti C (2012c) Braincase of *Panphagia protos* (Dinosauria, Sauropodomorpha) J Vert Paleontol 32(sup1):70–82

McPhee BW, Choiniere JN (2018) The osteology of *Pulanesaura eocollum*: implications for the inclusivity of Sauropoda (Dinosauria). Zool J Linn Soc 182(4):830–861

McPhee BW, Yates AM, Choiniere JN, Abdala F (2014) The complete anatomy and phylogenetic relationships of *Antetonitrus ingenipes* (Sauropodiformes Dinosauria): implications for the origins of Sauropoda. Zool J Linn Soc 171(1):151–205

McPhee BW, Benson RB, Botha-Brink J, Bordy EM, Choiniere JN (2018) A giant dinosaur from the earliest Jurassic of South Africa and the transition to quadrupedality in early sauropodomorphs. Current Biol 28(19):3143–3151.e7. https://doi.org/10.1016/j.cub.2018.07.063

McPhee BW, Bonnan MF, Yates AM, Neveling J, Choiniere JN (2015) A new basal sauropod from the pre-Toarcian Jurassic of South Africa: evidence of niche–partitioning at the sauropodomorph-sauropod boundary? Sci Rep 5(1):1–12

McPhee BW, Bittencourt JS, Langer MC, Apaldetti C, Da-Rosa ÁAS (2020) Reassessment of *Unaysaurus tolentinoi* (Dinosauria: Sauropodomorpha) from the Late Triassic (early Norian) of Brazil with a consideration of the evidence for monophyly within non–sauropodan sauropodomorphs. J Sys Palaeontol 18(3):259–293

Müller RT (2020) Craniomandibular osteology of *Macrocollum itaquii* (Dinosauria: Sauropodomorpha) from the Late Triassic of southern Brazil. J Sys Palaeontol 18(10):805–841

Müller RT (2021) Olfactory acuity in early sauropodomorph dinosaurs. Hist Biol. https://doi.org/10.1080/08912963.2021.1914600

Müller RT, Garcia MS (2019) Rise of an empire: analysing the high diversity of the earliest sauropodomorph dinosaurs through distinct hypotheses. Hist Biol 32:1334–1339

Müller RT, Garcia MS (2020) A paraphyletic 'Silesauridae' as an alternative hypothesis for the initial radiation of ornithischian dinosaurs. Biol Lett 16:20200417

Müller RT, Langer MC, Cabreira SF, Sias-da-Silva S (2016a) The femoral anatomy of Pampadromaeus barberenai based on a new specimen from the Upper Triassic of Brazil. Hist Biol 28(5):656–665. https://doi.org/10.1080/08912963.2015.1004329

Müller RT, Langer MC, Dias-da-Silva S (2016b) Biostratigraphic significance of a new early sauropodomorph specimen from the Upper Triassic of southern Brazil. Hist Biol 29(2):187–202

Müller RT, Langer MC, Pacheco CP, Sias-da-Silva S (2017a) The role of ontogeny on character polarization in early dinosaurs: a new specimen from the Late Triassic of southern Brazil and its implications. Hist Biol 31(6):794–805

Müller RT, Pretto FA, Stefanello M, Silva-Neves E, Dias-da-Silva S (2017b) On a dinosaur axis from one of the oldest dinosaur–bearing sites worldwide. Acta Palaeontol Pol 62(3):543–548

Müller RT, Langer MC, Bronzati M, Pacheco CP, Cabreira SF, Dias-Da-Silva S (2018a) Early evolution of sauropodomorphs: anatomy and phylogenetic relationships of a remarkably well–preserved dinosaur from the Upper Triassic of southern Brazil. Zool J Linn Soc 184(4):1187–1248

Müller RT, Pretto F, Kerber L, Silva-Neves E, Dias-da-Silva S (2018b) Comment on 'A dinosaur missing–link? *Chilesaurus* and the early evolution of ornithischian dinosaurs'. Biol Lett 14(3):20170581

Müller RT, Langer MC, Dias-da-Silva S (2018c) An exceptionally preserved association of complete dinosaur skeletons reveals the oldest long–necked sauropodomorphs. Biol Lett 14(11):20180633

Müller RT, Ferreira JD, Pretto FA, Bronzati M, Kerber L (2020) The endocranial anatomy of *Buriolestes schultzi* (Dinosauria: Saurischia) and the early evolution of brain tissues in sauropodomorph dinosaurs. J Anat 238(4):809–827

Nesbitt SJ (2011) The early evolution of archosaurs: relationships and the origin of major clades. Bull Am Mus Nat Hist 2011(352):1–292

Nesbitt SJ, Chatterjee S (2008) Late Triassic dinosauriforms from the Post Quarry and surrounding areas, west Texas, USA. Neues Jahrb Geol Palaontol Abh 249:143–156

Nesbitt SJ, Ezcurra MD (2015) The early fossil record of dinosaurs in North America: a new neotheropod from the base of the Upper Triassic Dockum Group of Texas. Acta Palaeontol Pol 60(3):513–526

Nesbitt SJ, Barrett PM, Werning S, Sidor CA, Charig AJ (2013) The oldest dinosaur? A middle Triassic dinosauriform from Tanzania. Biol Lett 9(1):20120949. https://doi.org/10.1098/rsbl.2012.0949

Nesbitt SJ, Smith ND, Irmis RB, Turner AH, Downs A, Norell MA (2009) A complete skeleton of a Late Triassic saurischian and the early evolution of dinosaurs. Science 326(5959):1530–1533

Nesbitt SJ, Sidor CA, Irmis RB, Angielczyk KD, Smith RM, Tsuji LA (2010) Ecologically distinct dinosaurian sister group shows early diversification of Ornithodira. Nature 464(7285):95–98

Novas FE, Agnolin FL, Ezcurra MD, Müller RT, Martinelli AG, Langer MC (2021) Review of the fossil record of early dinosaurs from South America, and its phylogenetic implicances. J South Am Earth Sc 110:103341

Novas FE, Ezcurra MD, Chatterjee S, Kutty TS (2011) New dinosaur species from the Upper Triassic Upper Maleri and Lower Dharmaram formations of central India. Earth Environ Sci Trans R Soc Edinb 101(3–4):333–349

Novas FE (1996) Dinosaur Monophyly. J Vert Paleontol 16:723–741

Otero A, Pol D (2013) Postcranial anatomy and phylogenetic relationships of *Mussaurus patagonicus* (Dinosauria Sauropodomorpha). J Vert Paleontol 33(5):1138–1168

Otero A, Krupandan E, Pol D, Chinsamy A, Choiniere J (2015) A new basal sauropodiform from South Africa and the phylogenetic relationships of basal sauropodomorphs. Zool J Linn Soc 174(3):589–634

Pacheco C, Müller RT, Langer MC, Pretto FA, Kerber L, Silva SD (2019) *Gnathovorax cabreirai*: a new early dinosaur and the origin and initial radiation of predatory dinosaurs. PeerJ 7:e7963

Parry LA, Baron MG, Vinther J (2017) Multiple optimality criteria support Ornithoscelida. R Soc Open Sci 4(10) 170833

Pol D (2004) Phylogenetic relationshps of basal Sauropodomorpha. PhD thesis, Columbia University

Pol D, Escapa IH (2009) Unstable taxa in cladistic analysis: identification and the assessment of relevant characters. Cladistics 25:515–527

Pol D, Otero A, Apaldetti C, Martínez RN (2021) Triassic sauropodomorph dinosaurs from South America: The origin and diversification of dinosaur dominated herbivorous faunas. J South Am Earth Sci 107:103145

Pretto FA, Schultz CL, Langer MC (2015) New dinosaur remains from the Late Triassic of southern Brazil (Candelária Sequence *Hyperodapedon* Assemblage Zone). Alcheringa 39(2):264–273

Pretto FA, Veiga FH, Langer MC, Schultz CL (2017) A juvenile sauropodomorph tibia from the 'Botucaraí Hill' Late Triassic of Southern Brazil. Rev Bras Paleontol 19(3):407–414

Pretto FA, Langer MC, Schultz CL (2019) A new dinosaur (Saurischia: Sauropodomorpha) from the Late Triassic of Brazil provides insights on the evolution of sauropodomorph body plan. Zool J Linn Soc 185(2):388–416

Raath M (1996) Earliest evidence of dinosaurs from central Gondwana. Mem Queensl Mus 39:703–709

Remes K, Rauhut O (2005) The oldest Indian dinosaur *Alwalkeria maleriensis* Chaterjee revised: a chimera including remains of a basal saurischian. In Kellner AWA, Henriques DDR, Rodrigues T (eds) Boletim de Resumos do II Congresso Latino-americano de Paleontologia de Vertebrados, p218. Serie Livros 12, Museu Nacional, Rio de Janeiro

Rogers RR, Swisher CC III, Sereno PC, Forster CA, Monetta AM (1993) The Ischigualasto tetrapod assemblage (Late Triassic) and 40Ar/39Ar calibration of dinosaur origins. Science 260:794–797

Salgado L, Coria RA, Calvo JO (1997) Evolution of titanosaurid sauropods. I. Phylogenetic analysis based on the postcranial evidence. Ameghiniana 34:3–32

Schultz CL, Martinelli AG, Soares MB, Pinheiro FL, Kerber L, Horn BLD, Pretto FA, Müller RT, Melo TP (2020) Triassic faunal successions of the Paraná Basin, southern Brazil. J South Am Earth Sci 104:102846

Sereno PC (1998) A rationale for phylogenetic definitions, with application to the higher-level taxonomy of Dinosauria. Neues Jahrb Geol Palaontol Abh 210:41–83

Sereno PC (1999) The evolution of dinosaurs. Science 284(5423):2137–2147

Sereno PC (2007a) Basal Sauropodormorpha: historical and recent phylogenetic hypothesis, with comments on *Ammosaurus major* (Marsh, 1889). Spec Pap Palaeontol 77:261–289

Sereno PC (2007b) Logical basis for morphological characters in phylogenetics. Cladistics 23:565–587

Sereno PC, McAllister S, Brusatte SL (2005) TaxonSearch: a relational database for suprageneric taxa and phylogenetic definitions. PhyloInformatics 8:1–21

Sereno PC, Martínez RN, Alcober OA (2012). Osteology of *Eoraptor lunensis* (Dinosauria, Sauropodomorpha). Basal sauropodomorphs and the vertebrate fossil record of the Ischigualasto Formation (Late Triassic: Carnian-Norian) of Argentina. J Vert Paleontol 32(sup1):83–179.

Sereno PC, Forster CA, Rogers RR, Monetta AM (1993) Primitive dinosaur skeleton from Argentina and the early evolution of the Dinosauria. Nature 361:64–66

Smith ND, Makovicky PJ, Hammer WR, Currie PJ (2007) Osteology of *Cryolophosaurus ellioti* (Dinosauria: Theropoda) from the Early Jurassic of Antarctica and implications for early theropod evolution. Zool J Linn Soc 151(2):377–421

Sues HD, Nesbitt SJ, Berman DS, Henrici AC (2011) A late-surviving basal theropod dinosaur from the latest Triassic of North. America Proc R Soc Lond B Biol Sci 278(1723):3459–3464

Swofford DL, Begle DP (1993) User's manual for PAUP: phylogenetic analysis using parsimony, Version 3.1. Washington D.C.: Smithsonian Institution

Upchurch P (1997). Sauropodomorpha. In Currie PG, Padian K (eds) Encyclopedia of Dinosaurs Academic Press San Diego p658–660

Upchurch P, Barrett PM, Galton PM (2007) A phylogenetic analysis of basal sauropodomorph relationships: implications for the origin of sauropod dinosaurs. Spec Pap Palaeontol 77:57

Wang YM, You HL, Wang T (2017) A new basal sauropodiform dinosaur from the Lower Jurassic of Yunnan Province China. Sci Rep 7(1):1–11

Yates AM (2003) A definite prosauropod dinosaur from the lower Elliot Formation (Norian: Upper Triassic) of South Africa. Palaeontol Africana 39:63–68

Yates AM (2004) *Anchisaurus polyzelus* (Hitchcock): the smallest known sauropod dinosaur and the evolution of gigantism among sauropodomorph dinosaurs. Postilla 230:1–58

Yates AM (2007a) The first complete skull of the Triassic dinosaur *Melanorosaurus* Haughton (Sauropodomorpha: Anchisauria) Evolution and palaeobiology of early sauropodomorph dinosaurs. Spec Pap Palaeontol 77:9–55

Yates AM, (2007b) Solving a dinosaurian puzzle: the identity of *Aliwalia rex* Galton. Hist Biol 19(1):93–123

Yates AM, Kitching JW (2003) The earliest known sauropod dinosaur and the first steps towards sauropod locomotion. Proc R Soc Lond B: Biol Sci 270(1525):1753–1758

Zerfass H (2007) Geologia da Folha Agudo, SH.22-V-C-V, escala 1:100.000. Serviço Geológico do Brasil-CPRM

Zerfass H, Lavina EL, Schultz CL, Garcia AGV, Faccini UF, Chemale F Jr (2003) Sequence stratigraphy of continental Triassic strata of southernmost Brazil: a contribution to Southwestern Gondwana palaeogeography and palaeoclimate. Sediment Geol 161:85–180

Zhang QN, You HL, Wang T, Chatterjee S (2018) A new sauropodiform dinosaur with a 'sauropodan' skull from the Lower Jurassic Lufeng Formation of Yunnan Province China. Sci Rep 8(1):1–12